

## 博士論文

パーキンソン病の原因遺伝子産物 Parkin が  
異常ミトコンドリアによって活性化される仕組み

小谷野 史香

## Doctoral thesis

The molecular basis underlying activation of the  
Parkinson's disease related gene product, Parkin,  
by impaired mitochondria.

Fumika Koyano

## **Contents**

<b>1. Abbreviations</b>	<b>• • • 1</b>
<b>2. Abstract</b>	<b>• • • 4</b>
<b>3. Introduction</b>	<b>• • • 6</b>
<b>4. Materials and Methods</b>	<b>• • • 11</b>
<b>5. Results</b>	<b>• • • 21</b>
<b>6. Discussion</b>	<b>• • • 41</b>
<b>7. Acknowledgements</b>	<b>• • • 50</b>
<b>8. Legends to the figures</b>	<b>• • • 52</b>
<b>9. References</b>	<b>• • • 63</b>

## 1. Abbreviations

AAV	Adeno-associated virus
ACN	Acetonitrile
AMBC	Ammonium bicarbonate
ARJP	Autosomal recessive juvenile parkinsonism
Ash	homo-oligomerized protein assembly helper
ATP	Adenosine triphosphate
CBB	Coomassie brilliant blue
CCCP	Carbonyl cyanide <i>m</i> -chlorophenylhydrazone
CMV	Cytomegalovirus
DMEM	Dulbecco's modified Eagle's medium
DTT	Dithiothreitol
FBS	Fetal bovine serum
GFP	Green fluorescence protein
HA	Hemagglutinin
hAG	Homo-tetramer azami-green
HEK293T	Human embryonic kidney 293T
HECT	Homologous to the E6-AP carboxyl terminus
HKI	Hexokinase I
IBR	In between ring
IP	Immunoprecipitation
IPTG	Isopropyl $\beta$ -D-1-thiogalactopyranoside

kAc	Potassium acetate
KD	Kinase dead
MEF	Mouse embryonic fibroblast
Mfn2	Mitofusin 2
mtDNA	Mitochondrial DNA
MTS	Mitochondrial targeting sequence
NEAA	Non-essential amino acid
NEM	<i>N</i> -ethylmaleimide
N.S.	Not significant
PAGE	Polyacrylamide gel electrophoresis
PARL	Presenilin-associated rhomboid-like
PD	Parkinson's disease
PEI	Polyethylenimine
PINK1	PTEN-induced putative kinase 1
PRM	Parallel reaction monitoring
PTEN	Phosphatase and tensin homolog deleted from chromosome 10
RBR	Ring between ring
RING	Really interesting new gene
ROS	Reactive oxygen species
S.D.	Standard deviation
SEM	Standard error of the mean
SDS	Sodium dodecyl sulfate
SUMO	Small ubiquitin-like modifier
TFA	Trifluoroacetic acid

TFAM	Mitochondrial transcription factor A
TMD	Transmembrane domain
TOM	Translocase of outer mitochondrial membrane
Ub	Ubiquitin
Ubl	Ubiquitin like domain
VDAC	Voltage-dependent anion channels
WT	Wild type

## 2. Abstract

*PINK1* and *PARKIN* are causal genes for hereditary Parkinsonism. *PINK1* is a Ser/Thr kinase that specifically localizes on depolarized mitochondria, whereas Parkin is a ubiquitin ligase (E3) that catalyzes ubiquitin transfer to mitochondrial substrates. Recent studies have shown that *PINK1* and Parkin play a pivotal role in the quality control of mitochondria, and that dysfunction of either protein results in the accumulation of low-quality mitochondria that triggers neuronal death and ultimately early-onset familial Parkinsonism. Since neurons are destined to degenerate in *PINK1*/Parkin-associated Parkinsonism, it is imperative to investigate the functions of *PINK1* and Parkin in neurons. However, most studies investigating *PINK1*/Parkin have utilized non-neuronal cell lines. Here I show that the principal *PINK1* and Parkin cellular events that have been documented in non-neuronal lines in response to mitochondrial damage also occur in primary neurons. I found that dissipation of the mitochondrial membrane potential triggers phosphorylation of both *PINK1* and Parkin, promoting that Parkin translocates to depolarized mitochondria. Furthermore, Parkin's E3 activity is re-established concomitant with ubiquitin-ester formation at Cys431 of Parkin. As a result, mitochondrial substrates in neurons become ubiquitylated. These results underscore the relevance of the *PINK1*/Parkin-mediated mitochondrial quality control pathway in primary neurons, and shed further light on the underlying mechanisms of the *PINK1* and Parkin pathogenic mutations that predispose Parkinsonism *in vivo*. Secondly, I further focused on Parkin activation mechanism in the *PINK1* and Parkin pathway. *PINK1* acts as an upstream factor for Parkin and is essential for activation of the latent E3 activity of Parkin and for recruiting Parkin onto depolarized mitochondria. Recently, mechanistic insights into *PINK1*/Parkin-mediated mitochondrial quality control have been revealed, and

PINK1-dependent phosphorylation of Parkin has been reported. However, PINK1 function was not bypassed by phosphomimetic Parkin mutation, and how PINK1 accelerates the E3 activity of Parkin on damaged mitochondria is still obscure. Here I report that ubiquitin is the genuine substrate of PINK1. Ser65 of ubiquitin was phosphorylated by PINK1 *in vitro* and in cells, and a Ser65 phosphopeptide derived from endogenous ubiquitin was only detected in cells in the presence of PINK1 and following a decrease in mitochondrial membrane potential in PINK1-expressing cells. Surprisingly, phosphomimetic ubiquitin made PINK1 dispensable for activation of phosphomimetic Parkin mutant in cells, and phosphorylated recombinant ubiquitin activated phosphomimetic Parkin *in vitro*. The phosphorylation-dependent interaction between ubiquitin and Parkin suggests that phosphorylated ubiquitin unlocks autoinhibition for the catalytic cysteine. These results show that PINK1-dependent phosphorylation of both Parkin and ubiquitin are sufficient for full activation of Parkin E3 activity, and thus phosphorylated ubiquitin is a Parkin activator.

### 3. Introduction

Mitochondrial homeostasis plays a pivotal role in the maintenance of normal healthy cells, in particular post-mitotic cells such as neurons. Mitochondria are constitutively injured by endogenous and exogenous stresses, such as reactive oxygen species (ROS) and mitochondrial DNA (mtDNA) mutations. Defective mitochondria, if left unchecked, become an aberrant source of oxidative stress due to the generation of excessive ROS and compromise healthy mitochondria through inter-mitochondrial reciprocity via fusion and fission. Thus, to maintain the integrity and quality of mitochondria, cells establish a mitochondrial quality control system via the selective elimination of impaired mitochondrion <sup>1</sup>.

Parkinson's disease (PD) is one of the most pervasive neurodegenerative diseases. Although the cause of sporadic PD is likely complex, numerous evidences link mitochondrial dysfunction to its pathogenesis. A moderate deficit in mitochondrial activity following exposure to pesticides such as rotenone (a mitochondrial complex I inhibitor) and paraquat (an oxidative stressor) predisposes to PD <sup>2</sup>, and mutations/deletions of mtDNA in PD patients have repeatedly been reported <sup>3</sup>. *PINK1* (PTEN-induced putative kinase 1) and *PARKIN* are causal genes for hereditary (i.e., autosomal recessive) early-onset Parkinsonism and have been studied thoroughly since their identification (Fig. 1) <sup>4 5</sup>. Although the phenotype of the hereditary

early-onset Parkinsonism is not the same as sporadic PD completely, they share a major clinical feature <sup>6</sup>. Newly emergent evidences have shown that PINK1 and Parkin play a pivotal role in the quality control of mitochondria, and dysfunction of either likely results in the accumulation of low-quality mitochondria thereby triggering early-onset familial Parkinsonism (Fig. 2) <sup>7 8</sup>. According to the most recently proposed model, PINK1 selectively localizes to low-quality mitochondria by escaping mitochondrial membrane potential ( $\Delta\Psi_m$ )-dependent degradation and subsequently undergoes autophosphorylation-dependent activation <sup>9 10</sup>. Activated PINK1 then recruits the latent form of Parkin from the cytosol to the same low-quality mitochondria <sup>11 12 13 10</sup>. Concomitantly, Parkin is phosphorylated at Ser65 in a PINK1-dependent manner and the ubiquitin ligase (E3) activity of Parkin is activated in part <sup>11 14 15 16</sup>. Although the molecular mechanism underlying how a decrease in  $\Delta\Psi_m$  activates Parkin has yet to be completely elucidated, suppression of the auto-inhibitory mechanism <sup>17</sup> and ubiquitin-thioester formation at Cys431 of Parkin <sup>18 16</sup> are thought to be critical steps for up-regulating the E3 activity of Parkin. Once activated, Parkin ubiquitylates outer mitochondrial membrane substrates such as hexokinase I (HKI), MitoNEET/CISD1, mitofusin (Mfn), miro, and voltage-dependent anion channel (VDAC) <sup>1 19 20 21 22 23 24 25 26 27 28</sup>.

Ubiquitylation engages in the sequential transfer of an ubiquitin molecule through an enzymatic cascade consisting of an ubiquitin-activating enzyme (E1), ubiquitin-conjugating

enzyme (E2) and ubiquitin ligase (E3), and so an isopeptide bond is formed between the C-terminus of ubiquitin and  $\epsilon$ -amino group of a lysine residue of a substrate protein (Fig. 3a) <sup>29</sup>.

The E2-E3 combination controls the specificity of the target protein selected to be modified, the site of attachment to the substrate protein, the length of the ubiquitin chain, and type of lysine linkage (e.g. K11, 48, 63) made between the attached ubiquitin molecules. Four different classes of E3 ubiquitin ligases have been identified namely HECT, RING, U-box, and RBR (RING-IBR-RING) E3 ligases (Fig.3a right). The HECT E3 ligases play a direct role to ubiquitylate substrates by forming a catalytic thioester intermediate between the cysteine residue and C-terminus of ubiquitin. The RING and U-box E3 ligases function as scaffolds allowing for efficient ubiquitin transfer to the target protein by trap of both ubiquitin-charged E2 and substrate. There is also an important group of E3 ligases known as RBR E3 ligases, e.g. Parkin <sup>30 18 16</sup>. The RBR E3 ligases retain an auto-inhibitory mechanism <sup>17</sup> and use a hybrid mechanism that combines aspects from both RING and HECT E3 ligase functions to facilitate the ubiquitylation reaction.

The outer mitochondrial membrane proteins are ubiquitylated (Fig. 3b). As a consequence, damaged mitochondria become quarantined through decreased mitochondrial fusion, separated from the destination (e.g. presynaptic terminal) by a pause in kinesin-dependent anterograde trafficking, degraded via the proteasome and/or autophagy.

The cascading reactions underlying transduction of the “mitochondrial damage” signal mediated by PINK1 and Parkin remain a topic of vigorous research. As described above, critical elements of this signal have been recently elucidated; however, several caveats to the current findings are worth highlighting. The most glaring shortcoming is that neuronal studies of PINK1 and Parkin have been limited with almost all aspects of the PINK1/Parkin pathway revealed using non-neuronal cell types (e.g. HeLa cells, HEK cells, and MEFs). Moreover, a report by Sterky *et al.* seriously undermined the relevance of mitochondrial quality control mediated by PINK1/Parkin in neurons<sup>31</sup>. To address these issues, I examined whether the PINK1/Parkin pathway reported in non-neuronal cells is also observed in primary neurons. Here I show for the first time using mouse primary neurons that both PINK1 and Parkin are phosphorylated following dissipation of  $\Delta\Psi_m$ , and that the E3 activity of Parkin is up-regulated following ubiquitin-ester formation<sup>32</sup>.

Besides, PINK1 is a Ser/Thr kinase that specifically localizes on depolarized mitochondria<sup>33 7 8</sup> and is essential for activation of the latent E3 activity of Parkin<sup>11</sup>. Recently, mechanistic insights into PINK1/Parkin-mediated mitochondrial quality control have been revealed<sup>33 7 8</sup>, and PINK1-dependent phosphorylation of Parkin has been reported<sup>14 15 16</sup>. However, PINK1 function was not bypassed by phosphomimetic Parkin mutation<sup>16</sup>, and how PINK1 accelerates the E3 activity of Parkin on damaged mitochondria is still obscure. Here I report that ubiquitin

is the genuine substrate of PINK1 and phosphorylated ubiquitin functions as a Parkin activator<sup>34</sup>.

## **4. Materials and Methods**

### **Lentivirus**

*HA-PARKIN*, *GFP-PARKIN*, or *PINK1-Flag* genes were cloned into a lentiviral vector (pLenti-CMV puro DEST, a kind gift from Dr. Eric Campeau at Resverlogix Corp.). Lentivirus was prepared following Campeau's protocols<sup>35</sup>. Briefly, lentiviral particles were produced in HEK293T cells by transfection of the aforementioned lentiviral vectors using Lipofectamine 2000 (Life Technologies). A lentivirus-containing supernatant was collected 48 h after transfection, and concentrated to 10 x by ultracentrifugation at 37,000 x g for 2 h.

### **Primary neuron culture**

Mouse studies were approved by the Animal Care and Use Committee of Tokyo Metropolitan Institute of Medical Science. Mouse fetal brains were taken from C57BL/6 wild type or *PARKIN*<sup>-/-</sup> mouse embryos at E15-16. After removing meninges, brain tissue was dissociated into a single-cell suspension using a Sumilon dissociation solution (Sumitomo Bakelite, Japan). Cells were plated at a density of 3-4 x 10<sup>5</sup> cells/ml on poly-L-lysine (Sigma)-coated dishes with the medium containing 0.33x Sumilon nerve-culture medium (Sumitomo Bakelite), 0.67% FBS (Equitech-bio, USA), 0.67x Neurobasal medium, 0.67x B27 supplements, 0.67x Glutamax

(above three reagents are from Life Technologies), and 0.67% Pen-Strep. Three days after plating (at day 4), neurons were infected with lentivirus containing *HA-PARKIN*, *GFP-PARKIN* or *PINK1-Flag*. After 4 h of infection, the virus media were removed. Neurons were treated with CCCP (30  $\mu$ M) for 1-3 h at day 7, and then harvested for immunoblotting or subjected to immunofluorescence.

### **Cells, plasmids, and transfections**

HeLa cells and MEFs were cultured at 32 - 37 °C with 5 % CO<sub>2</sub> in Dulbecco's modified Eagle's medium (DMEM, Sigma) containing 1x nonessential amino acids (Gibco), 1x sodium pyruvate (Gibco), and 10% fetal bovine serum (Gibco). *PINK1*<sup>-/-</sup> MEFs stably expressing WT or mutant PINK1 were established as reported previously<sup>11</sup>. To generate HeLa cells stably expressing PINK1-3xFlag, HeLa cells transiently expressing mCAT1 were infected with recombinant retroviruses harboring PINK1-3xFlag. Recombinant retrovirus was made using PLAT-E cells as reported previously<sup>16</sup>. Plasmids for expressing WT or various mutants of Parkin and ubiquitin were as described previously<sup>11 16</sup> or were newly constructed by conventional methods. Plasmid transfections were performed using the transfection reagent FuGene6 (Roche) for HeLa cells and polyethylenimine (Polyscience) for *PINK1*<sup>-/-</sup> MEFs. To depolarize the mitochondria, cells were treated with 15 -30  $\mu$ M CCCP (Wako) for 2 - 3 hr.

### **Phos-tag assay**

To detect phosphorylated proteins via SDS-PAGE, 7.5, 12.5 or 15 % polyacrylamide gels containing 50  $\mu$ M phos-tag acrylamide (Wako chemicals) and 100  $\mu$ M  $\text{MnCl}_2$  were used. After electrophoresis, phos-tag acrylamide gels were washed with gentle shaking in transfer buffer containing 0.01 % SDS and 1 mM EDTA for 10 min and then incubated in transfer buffer containing 0.01 % SDS without EDTA for 10 min according to the manufacturer's protocol. Proteins were transferred to PVDF membranes and analyzed by conventional immunoblotting as follows.

### **Preparation of recombinant ubiquitin proteins**

For purification of recombinant His<sub>6</sub>-ubiquitin, *E. coli* Rosseta2 (DE3) (Novagen) bacterial cells transformed with plasmids encoding WT or mutant His<sub>6</sub>-ubiquitin were pre-cultured overnight at 37 °C in 20 mL of LB medium supplemented with 100  $\mu$ g/mL ampicillin and 24  $\mu$ g/mL chloramphenicol, and then transferred to 200 mL of fresh medium. After incubation for 2 hr at 37 °C, IPTG was added at a final concentration of 1 mM, and *E. coli* were further cultured for 6 hr at 37 °C. The cells were harvested, suspended in 40 mL of 20 mM Tris-HCl pH 7.5, and lysed by sonication. After centrifugation at 8,000 rpm for 10 min, the supernatant was

recovered and purified by conventional methods, dialyzed against buffer (50 mM Tris-HCl pH 7.5, 100 mM NaCl, and 10 % glycerol) and stored at -80 °C. Non-tagged ubiquitin, HA-ubiquitin, His<sub>6</sub>-ubiquitin harboring C-terminal G75A,G76A mutation, and SUMO-1 were purchased from Boston Biochem.

### **Immunoblotting (IB)**

To observe autoubiquitylation of GFP-Parkin (an indicator for the re-establishment of the latent E3 activity of Parkin) in IB, lysates of primary neuron cells, HeLa cells or MEFs were collected in TNE-N<sup>+</sup> buffer [150 mM NaCl, 20 mM Tris-HCl pH 8.0, 1 mM EDTA and 1 % NP-40] in the presence of 10 mM NEM, which protects ubiquitylated proteins from deubiquitylase activity.

For phosphorylation analysis in IB, lysates from primary neurons, MEFs or HeLa cells were collected in the presence of PhosSTOP (Roche) to inhibit phosphatase activity. To detect various proteins via IB, the anti-ubiquitin antibody P4D1 (Santa Cruz, 1:1,000), Z0458 (DAKO, 1:500), anti-SUMO-1 (GMP-1) antibody 21C7 (ZYMED, 1:500), anti-Parkin antibody PRK8 (Sigma, 1:1,000-2,000), CS2132 (Cell Signaling, 1:1,000), anti-Flag antibody 2H8 (Transgenic, 1:500), anti-Mfn2 antibody ab56889 (Abcam, 1:500), anti-Miro1 antibody RHOT1 (Sigma, 1:500), anti-HKI antibody C35C4 (Cell Signaling, 1:1,000), anti-PINK1 antibody BC100-494 (Novus, 1:1,000), anti-GFP antibody ab6556 (Abcam, 1:500), anti-VDAC1 antibody ab2

(Calbiochem, 1:1,000), anti-FoF1 antibody (gift from Dr. T. Ueno, 1:1,000), and anti-Tom70 antibody (gift from Dr. Otera) were used.

### **Immunofluorescence (IF)**

For IF experiments, Primary neurons and HeLa cells were fixed with 4 % paraformaldehyde, permeabilized with 50 µg/mL digitonin, and stained with a primary antibody [anti-β-Tubulin isotype 3 antibody SDL.3D10 (Sigma, 1:100), and. anti-GFP antibody ab6556 (Abcam, 1:500), anti-Flag antibody 2H8 (Transgenic, 1:500), anti-Tom20 antibody FL-145 (Santa Crus Biotech., 1:3,000), F-10 (Santa Crus Biotech., 1:200)] and a 1:2,000 dilution of the secondary antibody [Alexa Fluor 488- 568- or 647- conjugated anti-mouse or -rabbit IgG antibody, (Invitrogen)]. Cells were imaged using a laser-scanning microscope (LSM510, 780; Carl Zeiss, Inc.) and image brightness was adjusted in Photoshop (Adobe). For statistical analysis, subcellular localization of Parkin and ubiquitin were analyzed in > 100 cells across three experiments, and statistical significance was calculated using Student's *t*-test.

### **Cell-free reconstitution of GFP-Parkin autoubiquitylation**

HeLa cells expressing exogenous GFP-Parkin were suspended in cell-free assay buffer [20 mM HEPES-KOH (pH 7.5), 220 mM sorbitol, 10 mM Potassium acetate (KAc), 70 mM

sucrose] supplemented with a protease inhibitor cocktail minus EDTA (Roche). Cells were disrupted by passaging 30 times through a 25-gauge needle, and cell homogenates were centrifuged at 800 x g for 10 min at 4 °C to obtain a post-nuclear supernatant. Cytosolic fractions were collected by further centrifugation at 20,400 x g for 10 min at 4 °C. For isolation of mitochondria, HeLa cells or MEFs expressing PINK1-3xFlag were treated with 15 – 30 μM CCCP for 3 hr followed by homogenization in the aforementioned cell-free assay buffer. Post-nuclear supernatants were then obtained by centrifugation as described above, and mitochondria were pelleted by further centrifugation at 10,000 x g for 20 min at 4 °C. To perform the cell-free ubiquitylation assay, HeLa cytosolic fractions containing exogenous GFP-Parkin were incubated with isolated mitochondria supplemented with 5 mM MgCl<sub>2</sub>, 5 mM ATP, 2 mM DTT, and 1% glycerol at 30 °C for 2 hr. To demonstrate that phosphorylated ubiquitin activates Parkin, ubiquitin was phosphorylated beforehand using isolated mitochondria, subjected to ultracentrifugation at 20,400 x g for 10 min at 4 °C to deplete mitochondria, and treated at 90 °C for 10 min. HeLa cytosolic fractions containing exogenous GFP-Parkin were incubated with non-phosphorylated or phosphorylated ubiquitin (final concentration is 50 μg/ml) supplemented with 5 mM MgCl<sub>2</sub>, 5 mM ATP, 2 mM DTT, and 1% glycerol at 30 °C for 2 hr.

### **Immunoprecipitation (IP) of PINK1**

For IP experiments, mitochondria from HeLa cells stably expressing-PINK1-3xFlag were collected as described above, re-suspended in cell-free assay buffer [20 mM HEPES-KOH (pH 7.5), 220 mM sorbitol, 10 mM KAc, 70 mM sucrose], solubilized with 10 mg/mL digitonin (Wako) for 15 min at 4 °C, and reacted with agarose (Protein G Sepharose 4 Fast Flow, GE Life Sciences) conjugated with anti-Flag antibody 2H8 for 1 hr at 4 °C. The resulting immunoprecipitates were washed repeatedly with the same buffer and collected by centrifugation.

### ***In vitro* phosphorylation of ubiquitin**

To phosphorylate ubiquitin with depolarized mitochondria *in vitro*, CCCP-treated mitochondria were collected as described above and then incubated with recombinant His<sub>6</sub>-ubiquitin (final concentration of 40 ng/μl) in cell-free assay buffer [20 mM HEPES-KOH (pH 7.5), 220 mM sorbitol, 10 mM KAc, 70 mM sucrose] supplemented with 5 mM MgCl<sub>2</sub>, 5 mM ATP, 2 mM DTT, and 1% glycerol at 30 °C for 1 hr. The supernatants were subsequently subjected to centrifugation at 16,000 x g for 10 min to deplete mitochondria. To phosphorylate ubiquitin with immunoprecipitated PINK1 *in vitro*, IP-PINK1 was added to the aforementioned assay instead of depolarized mitochondria. For the *in vitro* kinase assay using [ $\gamma$ -<sup>32</sup>P] ATP,

immunoprecipitated PINK1-3xFlag was incubated with HA-ubiquitin (10  $\mu$ g) or His<sub>6</sub>-ubiquitin (WT or S65A; 30  $\mu$ g) and 100  $\mu$ M [ $\gamma$ -<sup>32</sup>P] ATP (5  $\mu$ Ci) in 30  $\mu$ l kinase buffer (20 mM Tris-HCl, pH7.5, 5 mM MgCl<sub>2</sub>, and 1 mM DTT) for 30 min at 30 °C. The reaction was stopped by adding Laemmli's sample buffer and boiled. One-third of the sample was subjected to 17% SDS-PAGE and CBB staining. Phosphorylated proteins were then visualized by autoradiography.

#### **LC-MS/MS analysis of ubiquitin**

Mass spectrometric analyses were performed as reported previously<sup>16 10 36</sup> with some modification. To identify ubiquitin phosphorylation sites, recombinant ubiquitin was reacted with isolated mitochondria from CCCP-treated and -untreated cells. Recombinant ubiquitin was then subjected to SDS-PAGE, stained with CBB, and in-gel trypsin digestion was carried out as reported previously<sup>36</sup>. Gels were extensively washed with Milli-Q water (Millipore), the bands of interest were excised, cut into 1 mm<sup>2</sup> pieces, and destained with 1 mL of 50 mM ammonium bicarbonate (AMBC) buffer containing 50 % acetonitrile (ACN) with agitation for 1 hr. A final 100 % ACN wash was performed to ensure complete gel dehydration. Trypsinization solution (20 ng/ $\mu$ L) was prepared by diluting modified sequencing grade trypsin (Promega) with 50 mM AMBC buffer, pH 8.0, containing 5 % ACN. The trypsin solution was

added to the gel pieces and incubated at 37 °C for overnight. Digests were quenched and extracted by addition of 50 µL of 50 % ACN and 0.1 % trifluoroacetic acid (TFA) mixture for 1 hr by shaking. The digested peptides were recovered into fresh Protein Loin tubes and an additional extraction was performed with 70 % ACN and 0.1 % TFA mixture for 30 min. The extracted peptides were concentrated to 20 µL by speed-vac. The concentrated peptides were prepared in 0.1 % TFA. The resultant peptides were analyzed on a nanoflow UHPLC instrument [Easy nLC 1000, Q-Exactive MS and nanoelectrospray ion source (Thermo Fisher Scientific)] with the raw data processed using Xcalibur (Thermo Fisher Scientific). MS spectra were analyzed using Protein Discoverer software version 1.3 (Thermo Fisher Scientific). The fragmentation spectra were searched against UniProt database with the MASCOT search engine. To quantify the phosphorylation of endogenous ubiquitin following mitochondrial membrane potential dissipation, PINK1-expressing or intact HeLa cells were treated with CCCP. Whole cell lysates were collected in TNE-N<sup>+</sup> lysis buffer, subjected to SDS-PAGE and stained with CBB. The high (> 55 kDa), middle (14-55 kDa) and low molecular weight fraction (3 - 14 kDa) of the gels (as shown in Fig. 8g) were excised and cut into 1 mm<sup>2</sup> pieces. In-gel digestion using trypsin and lysyl endopeptidase (Wako) was carried out as described above. The absolute level of phosphorylated ubiquitin in PINK1-expressing or intact HeLa cells was measured by parallel reaction monitoring (PRM), a MS/MS-based quantification

method <sup>36</sup>. The extracted peptides were spiked with 10 fmol AQUA peptides as standards (ESTLHLVLR and EpSTLHLVLR, SIGMA) and analysed by Q Exactive in targeted MS/MS mode. Data were processed by PinPoint software version 1.3 (Thermo Fisher Scientific).

## 5. Results

### **PINK1 and Parkin are phosphorylated upon dissipation of mitochondrial membrane potential ( $\Delta\Psi_m$ ) in mouse primary neurons**

PINK1 and Parkin have been shown to cooperate in the identification, labeling, and clearance of mitochondria with low  $\Delta\Psi_m$ . Dysfunction of either appears to cause an accumulation of low-quality depolarized mitochondria and production of excessive reactive oxygen species (ROS), which trigger familial Parkinsonism<sup>33 7 8</sup>.

The most upstream event during PINK1/Parkin-mediated quality control of mitochondria is the discrimination of damaged mitochondria from their healthy counterparts by PINK1 via quantitative and qualitative regulation. Specifically, PINK1 accumulates following a decrease in  $\Delta\Psi_m$  by escaping from the  $\Delta\Psi_m$ -dependent degradation pathway. Autophosphorylation of the accumulated PINK1 promotes the efficient retrieval and co-localization of Parkin to damaged mitochondria<sup>11 12 10</sup>. I investigated whether PINK1 accumulates and undergoes phosphorylation in response to a decrease of  $\Delta\Psi_m$  in mouse primary neurons similar to that described in non-neuronal cells. I first tried to detect the endogenous mouse PINK1, however, the currently available anti-PINK1

antibodies were unable to differentiate between *PINK1*<sup>+/+</sup> and *PINK1*<sup>-/-</sup> MEFs even following carbonyl cyanide *m*-chlorophenylhydrazone (CCCP) treatment. I thus used exogenous Flag-tagged human PINK1. At 3 days after dissection, primary neurons were infected with lentivirus encoding PINK1-Flag. Primary neurons expressing PINK1-Flag were then treated with 30  $\mu$ M CCCP, which depolarizes mitochondria by increasing inner-membrane permeability to H<sup>+</sup>. The exogenous PINK1 was detected as a doublet in immunoblotting of conventional handmade gels (Fig. 4a, upper panel). This higher molecular band appeared within 1 h of CCCP treatment and persisted for 3 h. To demonstrate the phosphorylation of PINK1 directly, I performed a phosphate-affinity SDS-PAGE using polyacrylamide gels conjugated with a 1,3-bis (bis (pyridine-2-ylmethyl) amino) propan-2-olato diMn (II) complex (referred hereafter as phos-tag). Phos-tag can capture phosphomonoester dianions (ROPO<sub>3</sub><sup>2-</sup>) and thus acrylamide-pendant phos-tag specifically retards the migration of phosphorylated proteins, which are visualized as slower-migrating bands compared with the corresponding non-phosphorylated proteins <sup>37</sup>. Phos-tag PAGE demonstrated the phosphorylation of PINK1 in response to  $\Delta\Psi_m$  dissipation (Fig. 4a, lower panel) concomitantly with doublet formation in normal gels (upper panel).

Previously, several groups including ours reported that the N-terminal Ubl domain of Parkin was also phosphorylated at Ser65 upon dissipation of  $\Delta\Psi_m$  in cultured cells<sup>14 15 16</sup>. To examine whether phosphorylation of Parkin also occurs in neurons, HA-Parkin was exogenously introduced into mouse primary neurons by lentivirus and the cells were treated with 30  $\mu$ M CCCP for 1 to 3 h. Phos-tag PAGE confirmed phosphorylation of Parkin within 1 h of treatment with the phosphorylation signal increasing in intensity over time (Fig. 4b, lower panel). I next checked whether Ser65 is the phosphorylation site utilized in Parkin. HA-Parkin containing either a S65A or S65E mutation was introduced into *PARKIN*<sup>-/-</sup> mouse primary neurons, which were used to prevent confounding effects from endogenous Parkin. In both mutant cell lines the more intense slower migrating band identified as phosphorylated Parkin in Phos-tag PAGE was absent (Fig.4c, a red asterisk), suggesting that Ser65 is the genuine Parkin phosphorylation site in mouse primary neurons.

**Parkin is recruited to depolarized mitochondria and its latent E3 activity is up-regulated upon a decrease in mitochondrial membrane potential in neurons**

Parkin is selectively recruited to dysfunctional mitochondria with low membrane

potential in mammalian cell lines <sup>38</sup>. Moreover, our group previously demonstrated that the E3 function of Parkin in cultured cells (e.g. HeLa cells and MEFs) is activated upon dissipation of  $\Delta\Psi_m$  <sup>11</sup>. Parkin translocation onto neuronal depolarized mitochondria, however, is controversial. Mitochondrial transcription factor A (TFAM) is an essential protein that is an indispensable part of the basal transcription machinery for mtDNA. In addition, TFAM also regulates mtDNA copy number. Loss of TFAM results in mtDNA depletion and abolishes mtDNA expression, causing serious respiratory chain deficiency. Sterky *et al.* and Van Laar *et al.* reported that Parkin failed to localize on depolarized mitochondria following CCCP treatment <sup>39</sup> or by the loss of TFAM <sup>31</sup>, whereas Cai *et al.* and Joselin *et al.* reported that Parkin relocates to depolarized mitochondria in primary neurons <sup>40 41</sup>. I thus first examined whether Parkin is recruited to mouse primary neuron mitochondria following CCCP treatment. Neurons were infected with lentivirus encoding GFP-Parkin, and the subcellular localization of Parkin was examined in conjunction with immunofluorescence staining of Tom20 (a mitochondrial outer membrane marker) and  $\beta$ -tubulin isotype 3 (a neuron-specific marker). Under these experimental conditions, Parkin dispersed throughout the cytoplasm under steady-state conditions, whereas Parkin greatly co-localized with

depolarized mitochondria ( $t = \sim 3$  h) after treatment with CCCP (Fig. 5a). I next assessed the E3 activity of Parkin in primary neurons. GFP-Parkin can be ubiquitylated as a pseudosubstrate by Parkin in cells<sup>42 11</sup>. This electrophoretic pattern is characteristic of the autoubiquitylation of GFP-Parkin. As a consequence, autoubiquitylation of GFP-Parkin can be used as an indicator of Parkin E3 activity. As shown in Fig. 5b, autoubiquitylation of GFP-Parkin clearly increased following a decrease in  $\Delta\Psi_m$ , suggesting that latent E3 activity of Parkin is activated upon mitochondrial damage in neurons as previously reported in cultured cell lines (e.g. HeLa cells).

### **Pathogenic mutations impair the E3 activity of Parkin and inhibit localization to depolarized mitochondria**

To further verify that the events shown in Fig. 5 are etiologically important, I selected six pathogenic mutants of Parkin (K211N, T240R, R275W, C352G, T415N, and G430D) and examined their subcellular localization and E3 activity. To eliminate the effect of endogenous Parkin, I used primary neurons derived from *PARKIN*<sup>-/-</sup> mice in these experiments. The six GFP-Parkin mutants were serially introduced into *PARKIN*<sup>-/-</sup> primary neurons using a lentivirus and assayed for

their sub-cellular localization following CCCP treatment. Parkin mitochondrial localization was compromised by the K211N (mutation in RING0 domain), T240R (in RING1 domain), C352G (in IBR domain), T415N and G430D (both in RING2 domain) mutations (Fig. 6a). The defects seen with the K211N, T240R, C352G, and G430D mutants (Fig. 6b) were statistically significant ( $P < 0.01$ ). T415N seems to show a variation when compared to WT, although it was not statistically significant because of high divergence ( $P > 0.01$ ). The R275W mutation had no effect on mitochondrial localization following CCCP treatment. The E3 activity of the mutants was also assessed. The K211N, T240R, C352G, T415N and G430D mutations exhibited deficient autoubiquitylation activity in *PARKIN*<sup>-/-</sup> primary neurons (Fig. 6c). The R275W mutant had weak but reproducible autoubiquitylation activity following CCCP treatment. Because this mutant showed partial mitochondrial localization following CCCP treatment even in HeLa cells<sup>43 18</sup>, it is not surprising that the R275W mutant localizes to neuronal depolarized mitochondria and possesses weak E3 activity. Unexpectedly, the R275W mutant also localized to mitochondria even in the absence of CCCP treatment. Although the significance of R275W localization to healthy mitochondria is unknown, I propose that the R275W mutation causes unstable

structure and maintains Parkin in an inactive state (as suggested by Fig. 6c) because functional, phosphorylated PINK1 has not been reported on normal mitochondria. In most of the pathogenic Parkin mutants, translocation to damaged mitochondria and conversion to the active form were compromised following a decrease in  $\Delta\Psi_m$  (Fig. 6), suggesting the etiological importance of these events in neurons.

#### **Parkin forms an ubiquitin-thioester intermediate and ubiquitylates mitochondrial outer membrane proteins in mouse primary neurons**

Klevit's group recently reported that Cys357 in the RING2 domain of RBR-type E3 HHARI is an active catalytic residue and forms a ubiquitin-thioester intermediate during ubiquitin ligation <sup>30</sup>. Parkin is also a RBR-type E3 with Parkin Cys431 equivalent to HHARI Cys357. Various groups including us recently independently revealed that a Parkin C431S mutant forms a stable ubiquitin-oxyster upon CCCP treatment in non-neuronal cell lines, suggesting the formation of an ubiquitin-thioester intermediate <sup>18 16</sup>. To examine whether Parkin forms a ubiquitin-ester intermediate in neurons as well, I again used a lentivirus to express HA-Parkin with the C431S mutation, which converts an unstable

ubiquitin-thioester bond to a stable ubiquitin-oxyster bond. The HA-Parkin C431S mutant specifically exhibited an upper-shifted band equivalent to an ubiquitin-adduct following CCCP treatment (Fig. 7a, lane 4). This modification was not observed in wild type HA-Parkin (lane 2) and was absent when HA-Parkin with C431F pathogenic mutation which could not form ester-bond (lane 6). It suggests that Parkin is activated through its ubiquitin-oxyster formation when neurons are treated with CCCP

Next, I examined whether specific mitochondrial substrates undergo Parkin-mediated ubiquitylation in primary neurons. The ubiquitylation of Mfn1/2, Miro1, Tom20, Tom70, VDAC1, and hexokinase I (HKI) <sup>19 20 44 21 22 23 45 46 24 24 26 33 27</sup> <sup>28</sup> were evaluated by Western blotting. In initial experiments using primary neurons, detection of the ubiquitylated mitochondrial substrates (e.g. Mfn) was minimal. I thus changed various experimental conditions and determined that ubiquitylation of mitochondrial substrates became detectable when the primary neurons were cultured in media free of insulin, transferrin, and selenium (described in detail in Materials and Methods). Although these compounds are routinely added to the neuronal medium as antioxidants to reduce excessive ROS in primary neurons, their exclusion facilitated the detection of ubiquitylated

mitochondrial substrates (see Discussion). Higher molecular mass populations of endogenous Mfn1/2, Miro1, HKI, and VDAC1 were observed following CCCP treatment, this was particularly evident in neurons expressing exogenous Parkin (Fig. 7b). The modification resulted in a 6-7 kDa increase in the molecular weight, implying ubiquitylation by Parkin, as has been reported previously in non-neuronal cells. Moreover, in *PARKIN*<sup>-/-</sup> primary neurons, the modification of Mfn2 was not observed following CCCP treatment (Fig. 7c, compare lane 2 with 4), confirming that Mfn undergoes Parkin-dependent ubiquitylation in response to a decrease in  $\Delta\Psi_m$ .

### **Ubiquitin Ser65 is phosphorylated when $\Delta\Psi_m$ is decreased**

As aforementioned, mechanistic insights into PINK1/Parkin-mediated mitochondrial quality control have recently been revealed, however, one of the most poorly understood events is how the E3 activity of Parkin is accelerated by damaged mitochondria. PINK1 is essential for both the activation of latent E3 Parkin activity<sup>11</sup> and recruiting Parkin onto mitochondria following a decrease in  $\Delta\Psi_m$ <sup>11 12 20 13 22</sup>. Because PINK1 is a Ser/Thr protein kinase, the simplest model is that PINK1-dependent phosphorylation of Parkin accelerates its enzymatic

activity. Consistent with this model, our group and other researchers showed that Parkin is phosphorylated at Ser65 following a decrease in  $\Delta\Psi_m$  in a PINK1-dependent manner<sup>14 15 16</sup>. Furthermore, a phosphorylation-deficient mutation (S65A) of Parkin hindered the ubiquitin-ester intermediate formation necessary for Parkin activation, whereas a phosphomimetic mutation (S65E) partially bypassed the phosphorylation-dependency of Parkin activation<sup>16</sup>. However, the prerequisite for PINK1 was not bypassed by the phosphomimetic Parkin. I thus speculated that Parkin is not the sole PINK1 substrate and that phosphorylation of other PINK1 substrate(s) is imperative.

The structure of the N-terminal Parkin Ubl (ubiquitin-like) domain resembles that of ubiquitin<sup>47</sup>, and Ser65, the PINK1 phosphorylation site, is conserved in both proteins (Fig. 8a). Moreover, ubiquitin is a major component in the PINK1/Parkin pathway, and physical interactions between Parkin and ubiquitin have been suggested<sup>17 48</sup>. Namely, Zheng X *et al.* confirmed the interaction by the pull down assay<sup>48</sup>, and Changule V K *et al.* verified it by the peptide array method<sup>17</sup>. I thus examined whether ubiquitin is phosphorylated by PINK1. To detect a potentially phosphorylated ubiquitin, I performed phosphate-affinity (Phos-tag) PAGE in which the phosphorylated form of ubiquitin can be easily distinguished from the

non-phosphorylated form as a slower migrating band <sup>37</sup>. When PINK1-expressing HeLa cell lysates treated with CCCP were subjected to Phos-tag PAGE and immunoblotted using an anti-ubiquitin antibody, one retarded-mobility band with a small molecular weight was specifically observed in the CCCP-treated cell lysate (Fig. 8b), suggesting ubiquitin phosphorylation. To test whether depolarized mitochondria possess ubiquitin-phosphorylation activity, recombinant ubiquitin was incubated with ATP and Mg<sup>2+</sup> in the presence of isolated mitochondria from CCCP-treated or untreated cells. Ubiquitin phosphorylation was specifically observed in the reaction containing CCCP-pretreated mitochondria (Fig. 8c, lane 4). In contrast, the small ubiquitin-related modifier-1 (SUMO-1) protein, which has a ubiquitin-fold structure, was not phosphorylated by depolarized mitochondria (Fig. 8c, lane 8), suggesting that phosphorylation of ubiquitin is specific.

To determine the phosphorylation site, the phosphorylated ubiquitin obtained as Fig. 8c was trypsinized and subjected to LC-MS/MS analysis. Two phosphorylated ubiquitin peptides, 55-72 (TLSDYNIQKEpSTLHLVLR) and 64-72 (EpSTLHLVLR) were identified with high confidence, suggesting Ser65 of ubiquitin is phosphorylated (Fig. 8d). These phosphorylated peptides were not detected in control reactions containing mitochondria without CCCP treatment. To confirm

this, I purified recombinant 6xHis-tagged ubiquitin in which Ser65 was substituted with either Ala or Asp. When these ubiquitin mutants were subjected to Phos-tag PAGE following incubation with depolarized mitochondria *in vitro*, their phosphorylation was completely compromised by the Ser65 mutations (Fig. 8e). Mutating Ser65 of Flag-ubiquitin to Ala also prevented the band shift following CCCP treatment in Phos-tag PAGE (Fig. 8f). Importantly, when whole-cell extracts of PINK1-expressing HeLa cells were subjected to LC-MS/MS analysis, the non-phosphorylated ESTLHLVLR peptide of endogenous ubiquitin was detected in all conditions whereas the Ser65 phosphopeptide (EpSTLHLVLR) was detected only in CCCP-pretreated cells (Fig. 8g), confirming that Ser65 of ubiquitin is phosphorylated in cells. The absolute levels of phosphorylated ubiquitin of PINK1-expressing HeLa cell lysates were then determined using absolute quantification (AQUA) peptides as internal standards. Absolute quantification revealed that approximately 3% of total endogenous ubiquitin in low fraction was phosphorylated in PINK1-expressing cells following a decrease in mitochondrial membrane potential ( $\Delta\Psi_m$ ).

### **PINK1 phosphorylates ubiquitin**

I next investigated whether PINK1, which accumulates and is activated by CCCP treatment<sup>11 12 27 49</sup>, is involved in ubiquitin phosphorylation. When mitochondria derived from *PINK1* knockout (*PINK1*<sup>-/-</sup>) mouse embryonic fibroblasts (MEFs)<sup>50</sup> were used, ubiquitin phosphorylation was completely impeded even following CCCP pretreatment (Fig. 9a, lane 2). Expression of wild type (WT) PINK1 followed by CCCP treatment to trigger PINK1 activation<sup>10 49 10</sup> complemented the phosphorylation of ubiquitin (lane 4), confirming that PINK1 is essential for this process. Mitochondria from *PINK1*<sup>-/-</sup> MEFs harboring PINK1 mutants with loss of or decreased kinase activities [kinase-dead (KD), A168P, and G386A]<sup>10</sup> did not support phosphorylation of ubiquitin (Fig. 9a, lanes 6, 8, and 10). To demonstrate PINK1-catalyzed ubiquitin phosphorylation more convincingly, PINK1 immunoprecipitated from CCCP-treated and digitonin-solubilized mitochondria was tested *in vitro*. Immunoprecipitated PINK1 (referred to as IP-PINK1 hereafter) was free from obvious contamination of other mitochondrial proteins tested such as VDAC, mitofusin2, and FoF1 ATPase (Fig. 9b). Ubiquitin phosphorylation following incubation with the purified PINK1 was equivalent to that of CCCP-pretreated mitochondria (Fig. 9c). Moreover, when recombinant ubiquitin was incubated with IP-PINK1 and [ $\gamma$ -<sup>32</sup>P] ATP, incorporation of <sup>32</sup>P

was detected in the recombinant WT ubiquitin (Fig. 9d) but not the S65A ubiquitin mutant (Fig. 9e, lane 4). Taken together, these results demonstrate that PINK1 can directly phosphorylate ubiquitin at Ser65 without involvement of other protein kinases.

### **Mass-spectrometry-based absolute quantification of phosphorylated ubiquitin in intact HeLa cells**

Because the data presented above were derived from PINK1-overproducing cells, I next quantified ubiquitin phosphorylation in intact HeLa cells (Fig.10) and revealed that 0.05% of total endogenous ubiquitin in low fraction is phosphorylated (Fig. 10b, low fraction). Although the absolute level was very low, such a small fraction might be a significant pool dedicated to the PINK1 and Parkin pathway, as ubiquitin is pleiotropic.

### **Phosphomimetic ubiquitin activates phosphomimetic Parkin**

I next investigated the role of phosphorylated ubiquitin. PINK1 is essential for both activation of the latent E3 activity of Parkin <sup>11</sup> and recruiting Parkin onto depolarized mitochondria <sup>11 12 20 13 22</sup>. If ubiquitin is the genuine PINK1 substrate,

a phosphomimetic ubiquitin mutant would be expected to bypass the PINK1-dependency of the aforementioned events. To monitor restoration of the latent E3 activity of Parkin, autoubiquitylation of GFP-Parkin was used as an index <sup>11</sup>. In my first trial, expression of phosphomimetic ubiquitin mutant S65D led to neither mitochondrial localization (Figs. 11a, b) nor autoubiquitylation of GFP-Parkin (Fig. 11c, lane3). However, the CCCP treatment control triggered both mitochondrial localization (Fig. 11a) and autoubiquitylation (Fig. 11c, lane 4-6) of GFP-Parkin. Because PINK1 phosphorylates Parkin <sup>14 15 16</sup> in addition to ubiquitin, I used a phosphomimetic Parkin mutant Parkin(S65E) <sup>16</sup> in case both phosphorylation events are imperative. Even when the phosphomimetic GFP-Parkin(S65E) mutant was used, its cytoplasmic localization remained unchanged following co-expression with the phosphomimetic ubiquitin(S65D) mutant (Figs. 11d and 11e), whereas CCCP treatment stimulated translocation of GFP-Parkin(S65E) to mitochondria (Fig. 11d). In sharp contrast, phosphomimetic ubiquitin(S65D) promoted autoubiquitylation of GFP-Parkin(S65E) even in the absence of CCCP treatment (Fig. 11f, lane 3). Because phosphomimetic ubiquitin(S65D) and Parkin(S65E) did not localize on mitochondria (Fig. 11g), phosphomimetic ubiquitin stimulates the E3 activity of Parkin in the absence of

mitochondrial localization. Moreover, overproduction of phosphorylation deficient ubiquitin (Ser65Ala) delayed CCCP-triggered Parkin activation as compared with phosphorylatable wild-type ubiquitin, suggesting that the unphosphorylatable ubiquitin mutant competed with endogenous ubiquitin and thus exerted a dominant-negative effect (Fig.11h). Recently, it was noted that the Parkin W403A mutation weakened auto-inhibition and accelerated E3 activity<sup>51</sup>. When GFP-Parkin(W403A) was co-expressed with ubiquitin(S65D), its autoubiquitylation was also observed even without CCCP treatment (Fig. 11i, lane 3). These results suggest phosphorylated ubiquitin functions as a Parkin activator; otherwise Parkin is a unique E3 that exclusively recognizes phosphorylated ubiquitin for conjugation and thus catalyzes phospho-ubiquitylation. To investigate this, I replaced the phosphomimetic C-terminal diglycine motif, which is crucial for formation of the thioester intermediate during the cascading ubiquitylation reaction, with either Val or Ala (G75V/G76V and G75A/G76A). As shown in Fig. 11j, phosphomimetic ubiquitin with the diglycine mutations still triggered the E3 activity of GFP-Parkin(S65E) and GFP-Parkin(W403A) (Fig. 11j, lanes 5, 6, 11, 12; note that ubiquitylation bands in lanes 4 and 10 are slightly shifted upward by conjugation of exogenous Flag-ubiquitin(S65D), whereas bands

in lanes 5, 6, 11, and 12 are downward because only endogenous ubiquitin can conjugate). Moreover, Parkin catalyses conjugation of phosphorylation-deficient ubiquitin (S65A) to depolarized mitochondria following CCCP treatment as well as WT ubiquitin (Figs. 11k.l), indicating that Parkin does not exclusively recognize phospho-ubiquitin for ubiquitylation. Meanwhile, phosphomimetic ubiquitin could be conjugated to mitochondria and mitofusin-2 (Figs. 12a,b) in a CCCP-dependent manner. Thus, Parkin seems to conjugate both unphosphorylated and phosphorylated ubiquitin to the substrate.

I further confirmed the hypothesis that phosphorylated ubiquitin functions as a Parkin activator in a cell-free assay using GFP-Parkin and purified mitochondria<sup>16, 18</sup>. Autoubiquitylation of GFP-Parkin in intact cell extracts was specifically observed when incubated with CCCP-pretreated mitochondria, and was never observed in the reaction containing undamaged mitochondria or CCCP-pretreated mitochondria derived from *PINK1*<sup>-/-</sup> MEFs<sup>16, 18</sup>. Consistent with our previous results, autoubiquitylation of GFP-Parkin was not observed in the absence of depolarized mitochondria (Fig. 13a, lanes 2). In contrast, autoubiquitylation of GFP-Parkin mutants harboring the S65E or W403A mutations was clearly observed when incubated with recombinant phosphomimetic ubiquitin(S65D) in

the absence of depolarized mitochondria (Fig. 13a, lanes 12 and 18). WT ubiquitin and the phosphorylation-deficient S65A mutant did not support autoubiquitylation of Parkin S65E or W403A (lanes 7-10 and 13-16), and ubiquitin(S65D) did not accelerate autoubiquitylation of WT GFP-Parkin (lane 6). To rule out the possible effect of PINK1 contamination, I repeated the experiments using GFP-Parkin prepared from *PINK1*<sup>-/-</sup> MEFs. Autoubiquitylation of both S65E and W403A mutants of GFP-Parkin were again observed (Fig. 13b), further supporting that phosphomimetic ubiquitin makes PINK1 dispensable for phosphomimetic Parkin activation.

Finally, I used phosphorylated ubiquitin to more directly confirm Parkin activation. Ubiquitin was phosphorylated by incubation with depolarized mitochondria, then subjected to ultracentrifugation to deplete mitochondria, and finally treated at 90 °C for 10 min. Ubiquitin is a rare heat-stable protein and resistant to 90 °C treatment<sup>52</sup>, whereas any contaminating PINK1 would be inactivated under these conditions. The phosphorylated ubiquitin induced clear autoubiquitylation of GFP-Parkin(S65E) and GFP-Parkin(W403A) (Fig. 13c, lanes 4 and 6), indicating that phosphorylated ubiquitin activates Parkin *in vitro*. Similarly, when ubiquitin harboring the G75A/G76A mutation was phosphorylated beforehand and

incubated with a GFP-Parkin(S65E)-containing lysate, autoubiquitylation of GFP-Parkin(S65E) was observed (Fig. 13d, lane 6; note that mutant ubiquitin cannot conjugate to Parkin, the conjugation-competent endogenous ubiquitin is supplied in the Parkin-containing lysate), whereas ubiquitin(G75A/G76A) without phosphorylation did not promote autoubiquitylation (lane 4). These results confirmed that phosphorylated ubiquitin activates Parkin(S65E) independent of its conjugation activity (Fig. 11j). I next examined whether phosphorylated ubiquitin interacts physically with Parkin. Using the FluoPPI (fluorescent-based technology detecting protein-protein interactions) technique, in which the protein-protein interaction is detectable as foci formation in living cells, I demonstrated a clear interaction between Parkin and ubiquitin in cells. Importantly, Parkin with an intact Ubl domain failed to interact with phosphomimetic ubiquitin, whereas Parkin with a phosphomimetic (Ser65Glu) Ubl mutation could (Fig. 13e). This result suggests that the interaction between Parkin and phosphorylated ubiquitin competes with the intact Parkin Ubl domain, whereas phosphorylation of the Ubl domain releases this inhibitory effect.

In this study, I report that ubiquitin is the genuine substrate of PINK1. Ser65 of ubiquitin was phosphorylated by PINK1 *in vitro* and in cells, and a Ser65

phosphopeptide of endogenous ubiquitin was detected following a decrease in mitochondrial membrane potential. Unexpectedly, phosphomimetic ubiquitin bypassed PINK1-dependent activation of phosphomimetic Parkin mutant in cells, and phosphorylated recombinant ubiquitin activated phosphomimetic Parkin *in vitro*. These results show that, for the first time, PINK1-dependent phosphorylation of both Parkin and ubiquitin is sufficient for full activation of Parkin E3 activity, and thus phosphorylated ubiquitin is a Parkin activator.

## 6. Discussion

Recently, many reports on PINK1 and Parkin have contributed significantly to our understanding of their *in vivo* functionality. Most of these studies, however, have utilized non-neuronal cultured cell lines such as HeLa and HEK cells. To elucidate the physiological role of PINK1 and Parkin underlying the onset of hereditary Parkinsonism, evaluation of their role under more physiological conditions such as in neurons is imperative. I therefore sought to establish a mouse primary neuron experimental system to address this issue.

To isolate primary neurons from mouse brains, I first tried to dissociate neurons by 2.5% trypsin and treated with 1% DNaseI using previously reported protocol with minor modifications. Using this method,  $\sim 10^7$  cells were collected from fetal brains. In order to isolate more efficiently, I dissociated neurons by papain and suspended in culture medium using Sumilon dissociation solution. Collected neurons were dramatically increased to  $\sim 10^8$  cells. I succeeded in isolating neurons from brains stably and quickly with this method. Besides, primary neurons from adult brains failed to attach to the dish bottom and were unable to elongate their dendrites. Neurons should be handled very quickly and be kept cold to be collected

efficiently. Three days after plating neurons (corresponds to the birth period), contaminated latent proliferative cells (e.g. glial cells) were increasingly expanded. To avoid outgrowth of those populations, I treated with FUDR/uridine. Unexpectedly, both neurons and glial cells were severely damaged. Therefore, I started assay using primary neurons before proliferative cells expanded. Because isolated primary neurons tend to detach from the dish-bottom, I optimized the dish coating materials. As a result, gelatin and collagen did not exhibit any effect. The polyethylenimine- and poly-L-lysine- coated dish showed great impact to attach neurons to the dish-bottom. In general, it is well known that the gene transfection efficiency is extremely low in primary cells compared to cultured cells. I tried to optimize the transfection method for primary neurons. Firstly, I used the calcium phosphate and lipofectamine LTX (Life technologies) to transfect isolated primary neurons with GFP-plasmid, however they showed unstable and transient gene expression patterns. Also these compounds had toxicity to neurons. Secondly, I tried the electroporation methods using Neon transfection system (Life technologies) and NEPAGENE. Unfortunately, they were unable to introduce GFP-plasmid to primary neurons. Next, I used the GFP-integrated adenovirus or adeno-associated virus (AAV). Those viruses were prone to infect with glial cells

rather than neurons. Finally, I concluded that lentivirus showed the best transfection efficiency in primary neurons.

In my initial experiments, ubiquitylation of mitochondrial substrates (e.g. Mfn) in primary neurons following CCCP treatment was below the threshold of detection. I thus changed various experimental conditions including the composition and inclusion of supplementary factors to the culture medium. I determined that detection of ubiquitylation was improved when the primary neurons were cultured in media free of insulin, transferrin, and selenium. Transferrin plays a role in the reduction of toxic oxygen radicals, while selenium in the medium accelerates the anti-oxidant activity of glutathione peroxidase. Thus a weak oxidative stress to neuronal mitochondria seems to accelerate the ubiquitylation of mitochondrial substrates by Parkin. Because oxidative stress is assumed to be a primary stress for neuronal mitochondria *in vivo*<sup>53</sup>, this mechanism is thought to be critical for efficiently rescuing abnormal mitochondria under physiological conditions. Moreover, it has also been reported that oxidative stress helps Parkin exert for mitochondrial quality control in neurons<sup>41</sup>. Although the molecular mechanism underlying how weak oxidative stress accelerates Parkin-catalyzed ubiquitylation remains obscure, I speculate that deubiquitylase

activity in neuronal mitochondria conceals the ubiquitylation signal under steady state conditions. This activity is downregulated by oxidative stress <sup>54 55 56</sup>. Intriguingly, the Mfn2 ubiquitylation-derived signal in primary neurons remained fainter than that observed in cultured cells even using antioxidant-free media <sup>19 21</sup>. In this respect, I speculate that differences in the intracellular metabolic pathways between primary neurons and cultured cell lines affects ubiquitylation of mitochondrial substrates. Van Laar *et al.* reported that Parkin does not localize to depolarized mitochondria in cells forced into dependence on mitochondrial respiration e.g. galactose-cultured HeLa cells <sup>39</sup>. If so, ubiquitylation of mitochondrial substrates by Parkin would be less efficient because neurons have a higher dependency for mitochondrial respiration than other cultured cells.

In contrast to the ubiquitylation of mitochondrial substrates, I obtained clearer results concerning the other principal PINK1 and Parkin events following dissipation of  $\Delta\Psi_m$ , i.e. phosphorylation of PINK1 and Parkin (Fig. 4), translocation of Parkin to the depolarized mitochondria, and reestablishment of Parkin's E3 activity towards pseudo-substrates concomitant with ubiquitin-ester formation at Cys431 (Fig. 4-7). These data are consistent with what have been reported using non-neuronal cultured cells. In neurons, though the translocation of

Parkin onto damaged mitochondria is controversial. Initial efforts failed to detect Parkin localization to damaged neuronal mitochondria<sup>31-39</sup>. Subsequent studies, however, by two different groups in addition to me have successfully demonstrated the translocation event<sup>40-41</sup>. I suggest that methodological differences likely account for the seemingly conflicting observations. The study by Sterky *et al.* used adeno-associated virus encoding mCherry-Parkin that was delivered by stereotactic injections to midbrain dopaminergic neurons of *Tfam*-loss mice (MitoPark mice; genotype *Tfam*<sup>loxP/loxP</sup>;DAT-*cre*;ROSA26<sup>+lox-Stop-lox-mito-YFP</sup>)<sup>31</sup>, while Van Laar *et al.* used Lipofectamine 2000 to transfect wild type rat primary cortical neurons with human Parkin<sup>39</sup>. In contrast, I used primary neurons derived from *PARKIN*<sup>-/-</sup> mice infected with a lentivirus encoding GFP-Parkin to examine translocation of Parkin to damaged mitochondria. It is possible that the respective transfection efficiencies varied or that the methodological differences affected the neuronal cellular conditions, which may have impaired the behavior of exogenous Parkin. Alternatively, the presence of endogenous neuronal Parkin may account for the discrepancies. During my immunofluorescence experiments, I determined that mitochondrial localization of GFP-Parkin was more robust in *PARKIN*<sup>-/-</sup> neurons than wild type (*PARKIN*<sup>+/+</sup>) neurons suggesting that endogenous Parkin

is more efficiently translocated by the cellular machinery to depolarized-mitochondria than exogenous Parkin. Intriguingly, both the E3 activity and translocation of Parkin toward depolarized mitochondria were attenuated by disease-relevant Parkin mutations in primary neurons (Fig. 6). These results underscore the relevance of mitochondrial quality control mediated by PINK1/Parkin in neurons, and shed light on the mechanism by which pathogenic mutations of PINK1 and Parkin predispose to Parkinsonism *in vivo*.

In the present study, I also demonstrated – to my knowledge, for the first time – that Parkin activation in response to mitochondrial damage proceeded following ubiquitin phosphorylation by PINK1 in neurons. Previously, our group revealed that Parkin is kept latent under steady-state conditions<sup>11</sup>. Consistent with the model in this study, the structure of Parkin<sup>51 57 58 59</sup> revealed that the catalytic cysteine (Cys431) is occluded by the RING0 domain. The E3 activity of Parkin is usually repressed via auto-inhibition<sup>11 51 57 58</sup> but is specifically liberated by PINK1 in a unique two-step phosphorylation-dependent manner; i.e., one step is phosphorylation of the Ubl domain of Parkin<sup>14 15 16</sup> and another step is unexpectedly phosphorylation of ubiquitin (determined in this work).

To confirm the dependency of Parkin activation on ubiquitin phosphorylation, I

collaborated with Drs. Y. Tamura, T. Endo, and Y. Kimura and attempted to replace genomic ubiquitin with a phosphorylation-deficient mutant. However, this type of experiment is challenging because ubiquitin is encoded at four loci as fourteen copies in the human genome, and synthesized as a fusion protein with essential ribosomal subunits. As an alternative, we used a yeast system in which all the genomic-ubiquitin genes are disrupted, the fused ribosomal-proteins (L40 and S31) are complemented, and ubiquitin is expressed from a plasmid. So we introduced the S65A mutation into the yeast ubiquitin plasmid and co-expressed it with PINK1 and GFP-Parkin (note that yeast lack PINK1 and Parkin homologues). GFP-Parkin in yeast cells harboring WT ubiquitin underwent autoubiquitylation when co-expressed with WT PINK1, but lacked the modification when expressed with a kinase-dead (KD) PINK1 mutation or pathogenic Parkin mutations (Drs. Y. Tamura, T. Endo, and Y. Kimura; data not shown). In contrast, even when co-expressed with WT PINK1, GFP-Parkin did not show this modification in yeast only expressing the mutant ubiquitin (S65A) (data not shown). Taken together, the results obtained using this stringent heterologous cellular system strongly argue that ubiquitin phosphorylation at Ser65 is indeed essential for Parkin activation <sup>34</sup>. In addition, I also collaborated with Drs. E.A. Fon and J-F. Trempe to define the molecular

mechanism by which phosphorylated ubiquitin activates Parkin. We confirmed that phosphorylated ubiquitin was charged on UbcH7 as readily as non-phosphorylated ubiquitin, indicating a similar efficiency of conjugation by E1 and E2. We then examined whether phosphomimetic and phosphorylated ubiquitin accelerates discharging of UbcH7~unmodified ubiquitin in the presence of Parkin *in vitro* (note that the reaction does not contain E1 and ATP, thus free phosphorylated ubiquitin cannot enter into the conjugation pathway). Both phosphomimetic and phosphorylated ubiquitin accelerates discharging of ubiquitin from UbcH7~ubiquitin depending on catalytic cysteine (Cys431) of Parkin *in vitro*, revealing that the activation mechanism is strictly allosteric (Drs. E.A. Fon and J-F. Trempe; data not shown) <sup>34</sup> .

Together with the results presented in this study, I speculate that phosphorylation of both ubiquitin and Parkin Ubl domain unlocks repression of the catalytic cysteine by the RING0 domain for ubiquitin-thioester linkage, thereby converting Parkin to its fully-active form (Fig. 13g). To gain further insights in the mechanism, I collaborated with Dr. T. Hirokawa and generated two structural models by computational modeling that support binding of phosphorylated ubiquitin or phosphorylated Ubl domain facilitates accessibility to Cys431 as shown in (Dr. T.

Hirokawa; data not shown)<sup>34</sup>.

As mitochondrial dysfunction, especially complex I deficiency, has long been associated with sporadic PD<sup>60</sup>, a complete understanding of the molecular mechanism underlying Parkin activation is expected to clarify the pathogenesis of not only hereditary but also more common sporadic forms of PD. PD-related pathogenic PINK1 mutants which lost its kinase activity failed to phosphorylate ubiquitin. Without phosphorylated ubiquitin in cells, Parkin is not fully activated, and the impaired mitochondria are accumulated in neurons leading to the onset of PD. This study suggests that phosphorylated ubiquitin has a role to block PD. Moreover, although thousands of papers studying ubiquitin have been published, this work to my knowledge is the first to reveal ubiquitin phosphorylation and its significance.

## 7. Acknowledgements

I would like to thank Dr. Jie Shen (Harvard Medical School) for giving *PINK1<sup>-/-</sup>* MEFs, Dr. Toshio Kitamura (Tokyo University) for giving Plat-E cells. I thank Dr. Eric Campeau (Resverlogix Corp.) for providing lentivirus-packaging plasmids, Dr. Hidenori Otera (Kyushu University) for the anti-Tom70 antibody, and Drs. Haruo Okado and Chiaki Ohtaka-Maruyama (Tokyo Metropolitan Institute of Medical Science) for valuable advice. I also wish to acknowledge valuable discussions with Dr. Kei Okatsu (Tokyo Metropolitan Institute), Ms. Mayumi Kimura, Ms. Etsu Go, Dr. Shinshuke Ishigaki (Nagoya University Graduate School of Medicine), Dr. Gen Sobue (Nagoya University Graduate School of Medicine), Dr. Yushuke Fujioka (Nagoya University Graduate School of Medicine), Dr. Hidetaka Kosako (The University of Tokushima), Dr. Yasushi Tamura (Nagoya University), Dr. Takatsugu Hirokawa (National Institute of Advanced Industrial Science and Technology), Dr. Toshiya Endo (Kyoto Sangyo University), Dr. Edward A. Fon (McGill University), Dr. Jean-Francois Trempe (McGill University).

I appreciate the help from Dr. Yasushi Saeki (Tokyo Metropolitan Institute), Dr. Hidehito Yoshihara (Tokyo Metropolitan Institute) and Mr. Hikaru Tsuchiya

(Tokyo University) for mass-spectrometry technique.

Dr. Keiji Tanaka and Dr. Noriyuki Matsuda give insightful comments and suggestions.

## 8. Legends to the figures

**Figure 1: A history of PINK1/Parkin study**

**Figure 2: Mitochondrial energetic mechanism and the quality control system**

Mitochondria homeostasis plays a pivotal role in the maintenance of healthy cells.

Mitochondria are constitutively injured by endogenous and exogenous stresses, such as reactive oxygen species (ROS) and mitochondrial DNA (mtDNA) mutations.

Defective mitochondria become an aberrant source of oxidative stresses due to the generation of excessive ROS and compromise healthy mitochondria. Thus, to maintain the integrity and quality of mitochondria, cells establish a mitochondrial quality control system via the selective elimination of impaired mitochondrion.

Because PINK1/Parkin, the products of PD causal genes, play an important role in elimination of damaged mitochondria, the deletion or mutation in *PINK1/PARKIN* genes cause the accumulation of damaged mitochondrion in cells. As a consequence, it is thought that the accumulation of unhealthy mitochondrion in neurons leads to the onset of PD.

**Figure 3: Ubiquitylation and proteolysis systems**

a, The ubiquitin-activating enzyme (E1) activates ubiquitin in an ATP-dependent manner to form a thioester bond between the C-terminal carboxyl group of ubiquitin and the catalytic cysteine of the E1. The ubiquitin is then transferred to an ubiquitin-conjugating enzyme (E2) by transthiolation reaction to form a thioester bond between the C-terminus of ubiquitin and the conserved catalytic cysteine residue in the E2. The HECT E3 ligases interact with the ubiquitin-charged E2 via E2 N-terminal region and perform another transthiolation reaction to form a thioester bond between the C-terminus of ubiquitin and the conserved catalytic cysteine residue in the C-terminal region of the HECT E3s. This HECT~ubiquitin intermediates is then prepared for the subsequent transfer of ubiquitin to a substrate. The RING E3 ligases, the ubiquitin-charged E2 interacts with the RING domain of the E3, subsequently the ubiquitin transfers to a substrate protein. The RBR E3 ligases (e.g. Parkin) use a combination of the RING and HECT mechanisms (RING-HECT hybrid). In this mechanism, the RING1 engages with the ubiquitin-charged E2 in a similar manner to the RING E3s, while the RING2 acts in a similar fashion to the C-terminal region of the HECT E3s by performing a transthiolation reaction to form a thioester bond between the C-terminus of ubiquitin and the catalytic

cysteine in the RING2 domain of RBR E3s.

**b**, The outer mitochondrial membrane proteins are ubiquitylated and degraded via the proteasome and/or autophagy.

**Figure 4: PINK1 and Parkin are phosphorylated following a decrease in  $\Delta\Psi_m$  in mouse primary neurons.**

Neurons were infected with lentivirus encoding PINK1-Flag (**a**), wild type HA-Parkin (**b**), or HA-Parkin with either the S65A or S65E mutation (**c**). Cells were treated with the mitochondrial uncoupler CCCP (30  $\mu\text{M}$ ) for 1 to 3 h and subjected to SDS-PAGE in the absence or presence of 50  $\mu\text{M}$  phos-tag. Note that mobility does not reflect the molecular weight of proteins in Phos-tag PAGE<sup>61</sup> and thus molecular weight markers are not shown in the bottom gels. The red asterisks in (**b**) and (**c**) indicate phosphorylation of Parkin at Ser65.

**Figure 5: Parkin is recruited to depolarized mitochondria and is activated in neurons.**

**a**, Mouse primary neurons were infected with lentivirus encoding GFP-Parkin and then subjected to CCCP treatment (30  $\mu\text{M}$ ) for 3 h. Neurons were immunostained

with the indicated antibodies. Insets (white boxes) in the Parkin, Tom20, and  $\beta$ -tubulin 3 co-immunostained images have been enlarged to better show co-localization. **b**, The E3 activity of Parkin was monitored using autoubiquitylation of GFP-Parkin as an indicator. As reported previously <sup>11</sup>, Parkin ubiquitylates a pseudosubstrate (N-terminally fused GFP) only when the mitochondrial membrane potential decreases. Ub, ubiquitin.

**Figure 6: Disease-relevant Parkin mutations impair mitochondrial localization and E3 activity following CCCP treatment.**

**a**, The subcellular localization of GFP-Parkin with pathogenic mutations in the isolated neurons from *PARKIN* knock-out (*PARKIN*<sup>-/-</sup>) mice. Primary neurons were infected with lentivirus encoding GFP-Parkin containing various disease-relevant mutations and then treated with CCCP (30  $\mu$ M) for 3 h, followed by immunocytochemistry, as in Figure 5a. **b**, The number of neurons with GFP-Parkin-positive mitochondria was counted. Error bars represent the mean  $\pm$  S.D. values of two experiments. Statistical significance was calculated using analysis of variance with a Student's *t*-test. **c**, The E3 activity of Parkin with disease-relevant Parkin mutations. *PARKIN*<sup>-/-</sup> primary neurons expressing

pathogenic GFP-Parkin were treated with CCCP for 3 h, and subjected to immunoblotting with an anti-Parkin antibody.

**Figure 7: Several outer-membrane mitochondrial proteins underwent Parkin-dependent ubiquitylation following a decrease in the  $\Delta\Psi_m$ .**

**a**, Ubiquitin-oxyester formation on Parkin (shown by the red asterisk) was specifically observed in the Parkin C431S mutant following CCCP treatment in primary neurons. This modification was not observed in wild type Parkin or the C431F mutant. **b**, Intact primary neurons or primary neurons infected with lentivirus encoding Parkin were treated with CCCP and then immunoblotted to detect endogenous Mfn2, Miro1, HKI, VDAC1, Mfn1, Tom70, and Tom20. The red arrowheads and asterisks indicate ubiquitylated proteins. **c**, Ubiquitylation of Mfn2 following mitochondrial depolarization (shown by the red asterisk) is prevented by *PARKIN* knock-out in primary neurons.

**Figure 8: Ubiquitin Ser65 is phosphorylated when  $\Delta\Psi_m$  is decreased.**

**a**, Sequence comparison between human ubiquitin and the Parkin Ubl domain. **b**, HeLa cells stably expressing PINK1 following protonophore (CCCP) treatment

were subjected to Phos-tag PAGE and immunoblotted with an anti-ubiquitin (Ub) antibody. Red asterisk; putative phosphorylated ubiquitin. Ubn: ubiquitylated proteins. **c**, Recombinant ubiquitin was phosphorylated by depolarized mitochondria prepared from PINK1-expressing HeLa cells *in vitro*, but recombinant SUMO was not. Red asterisk indicates phosphorylated ubiquitin. **d**, Mass spectrometric (MS) analysis of the tryptic phosphopeptide from ubiquitin that was phosphorylated by depolarized mitochondria *in vitro*. The MS/MS data indicated that phosphorylation occurs at Ser65. **e** and **f**, Mutation of Ser65 prevents ubiquitin phosphorylation by damaged mitochondria *in vitro* (**e**) and following protonophore treatment in cells (**f**). Experiments were performed as in **c** and **b**, respectively. **g**, Portion of the gel corresponding to high, middle and low molecular weight fractions of whole-cell extracts used for MS analysis is shown (upper left panel). Absolute quantification of ESTLHLVLR and EpSTLHLVLR peptides in PINK1-expressing cells was calculated across three experiments (lower left graph and right graphs). Error bars represent the mean  $\pm$  SEM values. Statistical significance was calculated using a one-tailed paired *t*-test. (significant if  $P < 0.05$ ).

**Figure 9: PINK1 phosphorylates ubiquitin.**

**a**, PINK1 on depolarized mitochondria and its kinase activity are essential for ubiquitin phosphorylation *in vitro*. **b**, PINK1 was immunoprecipitated, and its purity was confirmed by immunoblotting with antibodies against other mitochondrial membrane proteins. **c**, Immunoprecipitated PINK1 (IP-PINK1) phosphorylates ubiquitin *in vitro* equivalent to depolarized mitochondria. **d** and **e**, Ubiquitin was labeled with  $^{32}\text{P}$  by IP-PINK1 prepared from CCCP-treated mitochondria (**d**), whereas the ubiquitin(S65A) mutant was not (**e**). Black asterisks indicate heavy and light chains of immunoglobulin in the IP-PINK1 preparations.

**Figure 10: Mass-spectrometry-based absolute quantification of phosphorylated ubiquitin in intact HeLa cells.**

**a**, Because the signal intensity is low, the original data and chromatogram of EpSTLHLVLR peptide are also shown. **b**, Whole cell lysates of intact HeLa cells  $\pm$  CCCP treatment were subjected to SDS-PAGE, and the high (>55 kDa), middle- (14-55kDa), or low (<14 kDa) molecular-weight fractions were collected. The absolute quantities of ESTLHLVLR and EpSTLHLVLR peptides in each fraction were then determined using AQUA peptides as standards in three experiments.

Error bars represent mean  $\pm$  SEM and statistical significance was calculated using a one-tailed paired *t*-test. **c**, The light signal (derived from endogenous EpSTLHLVLR peptide), which shows a similar ionized pattern and the identical elution time as the heavy signal (derived from internal AQUA EpSTLHLVLR control peptide), was observed only in CCCP-pretreated cells (red arrows).

**Figure 11: Phosphomimetic ubiquitin activates phosphomimetic Parkin.**

**a**, Localization of WT Parkin co-expressed with WT or phosphomimetic ubiquitin(S65D). Bars indicate 10  $\mu$ m. **b**, The rate of mitochondrial Parkin localization without CCCP treatment was 0% when calculated in 100 cells across three experiments. **c**, Autoubiquitylation of GFP-Parkin was not observed by co-expression of phosphomimetic ubiquitin (red vertical bars). **d** and **e**, Localization of the phosphomimetic Parkin(S65E) mutant co-expressing with WT or phosphomimetic ubiquitin. Immunocytochemistry (**d**) and statistical analysis (**e**) were performed as in **a** and **b**. **f**, Autoubiquitylation of phosphomimetic GFP-Parkin(S65E), evidence for the re-establishment of its E3 activity, was observed by co-expression of phosphomimetic ubiquitin(S65D) even in the absence of CCCP treatment (lane 3). **g**, Phosphomimetic ubiquitin (Ser65Asp) stimulates

the E3 activity of Parkin in the absence of mitochondrial localization. Example figures indicative of cytoplasmic localization of both phosphomimetic Parkin and ubiquitin are shown. Mitochondrial localization was 0% of 100 cells in two independent experiments. Bars indicate 10 $\mu$ m. **h**, co-expression of phosphorylation-deficient ubiquitin (Ser65Ala) mutant delayed CCCP-dependent activation of WT Parkin. **i**, Phosphomimetic ubiquitin(S65D) induced autoubiquitylation of GFP-Parkin(W403A). **j**, The C-terminal diglycine motif (GG) is dispensable for Parkin activation. Red asterisks indicate autoubiquitylation of the GFP-Parkin(S65E) and GFP-Parkin(W403A) mutants. **k**, Parkin mediated mitochondrial localization of phosphorylation-deficient ubiquitin(S65A) following a decrease in  $\Delta\Psi$ m. **l**, The rate of Flag-Ub on mitochondria was calculated as a percentage using 100 cells across three experiments. Error bars represent the mean  $\pm$  SEM values. N.S; not significant ( $P > 0.05$ ) in one-tailed Student's *t*-test.

**Figure 12: Subcellular localization of phosphomimetic or phosphorylation-deficient ubiquitin under various experimental conditions.**

**a**, Mitochondrial accumulation of phosphomimetic or phosphorylation-deficient ubiquitin depending on Parkin and CCCP treatment (3h). **b**, Phosphomimetic

ubiquitin (Ser65Asp) is conjugated to the Parkin substrate mitofusin-2. Red bars indicate ubiquitylation of mitofusin-2 with phosphomimetic Flag-ubiquitin (lane 2) or phosphorylation-deficient Flag-ubiquitin (lane4).

**Figure 13: Phosphorylated ubiquitin activates Parkin *in vitro*.**

**a**, Recombinant phosphomimetic ubiquitin(S65D) converts GFP-Parkin(S65E) and GFP-Parkin(W403A) mutants to the active form. **b**, GFP-Parkin mutants prepared from *PINK1*<sup>-/-</sup> MEFs still undergo autoubiquitylation following incubation with phosphomimetic ubiquitin(S65D). **c**, Recombinant ubiquitin, which was phosphorylated beforehand *in vitro*, was incubated with WT, S65E, and W403A GFP-Parkin from mitochondria-intact cells. **d**, Phosphorylated ubiquitin(G75A/G76A) lacking conjugation activity promoted autoubiquitylation of Parkin(S65E). **e**, FluoPPI assay revealed a physical interaction between phosphomimetic Parkin and phosphomimetic ubiquitin. A Cys431 Ala mutation of Parkin and a Gly75 Ala/Gly76 Ala mutation of ubiquitin prevented a ubiquitylation-derived pseudo positive signal. hAG-Ub, hAG (homo-tetramer Azami-Green)-tagged ubiquitin; Ash-Parkin, Ash (homo-oligomerized protein assembly helper)-tagged Parkin. **f**, Foci-containing cells were calculated in 100

cells across three experiments. Error bars represent the mean  $\pm$  SEM and statistical significance was calculated using a one-tailed paired *t*-test. **g**, A model for Parkin activation. PINK1 activates latent Parkin via two phosphorylation steps at Ser65 in both the Parkin Ubl domain and ubiquitin. Phosphorylation of each singly is insufficient for activity. Instead, both phosphorylation events are thought to de-repress the RING0 domain and relieve the catalytic cysteine (Cys431) of Parkin.

**Table 1: A list of the ubiquitin peptides used in parallel monitoring assay to quantify phosphorylated ubiquitin**

For each peptide, the optimal precursor ion and product ions are shown.

## 9. References

1. Ashrafi, G.; Schwarz, T. L., The pathways of mitophagy for quality control and clearance of mitochondria. *Cell death and differentiation* 2013, *20* (1), 31-42.
2. Tanner, C. M.; Kamel, F.; Ross, G. W.; Hoppin, J. A.; Goldman, S. M.; Korell, M.; Marras, C.; Bhudhikanok, G. S.; Kasten, M.; Chade, A. R.; Comyns, K.; Richards, M. B.; Meng, C.; Priestley, B.; Fernandez, H. H.; Cambi, F.; Umbach, D. M.; Blair, A.; Sandler, D. P.; Langston, J. W., Rotenone, paraquat, and Parkinson's disease. *Environmental health perspectives* 2011, *119* (6), 866-72.
3. Schapira, A. H., Mitochondria in the aetiology and pathogenesis of Parkinson's disease. *Lancet neurology* 2008, *7* (1), 97-109.
4. Kitada, T.; Asakawa, S.; Hattori, N.; Matsumine, H.; Yamamura, Y.; Minoshima, S.; Yokochi, M.; Mizuno, Y.; Shimizu, N., Mutations in the parkin gene cause autosomal recessive juvenile parkinsonism. *Nature* 1998, *392* (6676), 605-8.
5. Valente, E. M.; Abou-Sleiman, P. M.; Caputo, V.; Muqit, M. M.; Harvey, K.; Gispert, S.; Ali, Z.; Del Turco, D.; Bentivoglio, A. R.; Healy, D. G.; Albanese, A.; Nussbaum, R.; Gonzalez-Maldonado, R.; Deller, T.; Salvi, S.; Cortelli, P.; Gilks, W. P.; Latchman, D. S.; Harvey, R. J.; Dallapiccola, B.; Auburger, G.; Wood, N. W., Hereditary early-onset Parkinson's disease caused by mutations in PINK1. *Science* 2004, *304* (5674), 1158-60.
6. Imaizumi, Y.; Okada, Y.; Akamatsu, W.; Koike, M.; Kuzumaki, N.; Hayakawa, H.; Nihira, T.; Kobayashi, T.; Ohyama, M.; Sato, S.; Takanashi, M.; Funayama, M.; Hirayama, A.; Soga, T.; Hishiki, T.; Suematsu, M.; Yagi, T.; Ito, D.; Kosakai, A.; Hayashi, K.; Shouji, M.; Nakanishi, A.; Suzuki, N.; Mizuno, Y.; Mizushima, N.; Amagai, M.; Uchiyama, Y.; Mochizuki, H.; Hattori, N.; Okano, H., Mitochondrial dysfunction associated with increased oxidative stress and alpha-synuclein accumulation in PARK2 iPSC-derived neurons and postmortem brain tissue. *Molecular brain* 2012, *5*, 35.
7. Corti, O.; Lesage, S.; Brice, A., What genetics tells us about the causes and mechanisms of Parkinson's disease. *Physiological reviews* 2011, *91* (4), 1161-218.
8. Exner, N.; Lutz, A. K.; Haass, C.; Winklhofer, K. F., Mitochondrial dysfunction in Parkinson's disease: molecular mechanisms and pathophysiological consequences. *The EMBO journal* 2012, *31* (14), 3038-62.
9. Jin, S. M.; Lazarou, M.; Wang, C.; Kane, L. A.; Narendra, D. P.; Youle, R. J., Mitochondrial membrane potential regulates PINK1 import and proteolytic destabilization by PARL. *The Journal of cell biology* 2010, *191* (5), 933-42.

10. Okatsu, K.; Oka, T.; Iguchi, M.; Imamura, K.; Kosako, H.; Tani, N.; Kimura, M.; Go, E.; Koyano, F.; Funayama, M.; Shiba-Fukushima, K.; Sato, S.; Shimizu, H.; Fukunaga, Y.; Taniguchi, H.; Komatsu, M.; Hattori, N.; Mihara, K.; Tanaka, K.; Matsuda, N., PINK1 autophosphorylation upon membrane potential dissipation is essential for Parkin recruitment to damaged mitochondria. *Nature communications* 2012, *3*, 1016.
11. Matsuda, N.; Sato, S.; Shiba, K.; Okatsu, K.; Saisho, K.; Gautier, C. A.; Sou, Y. S.; Saiki, S.; Kawajiri, S.; Sato, F.; Kimura, M.; Komatsu, M.; Hattori, N.; Tanaka, K., PINK1 stabilized by mitochondrial depolarization recruits Parkin to damaged mitochondria and activates latent Parkin for mitophagy. *The Journal of cell biology* 2010, *189*(2), 211-21.
12. Narendra, D. P.; Jin, S. M.; Tanaka, A.; Suen, D. F.; Gautier, C. A.; Shen, J.; Cookson, M. R.; Youle, R. J., PINK1 is selectively stabilized on impaired mitochondria to activate Parkin. *PLoS biology* 2010, *8*(1), e1000298.
13. Vives-Bauza, C.; Zhou, C.; Huang, Y.; Cui, M.; de Vries, R. L.; Kim, J.; May, J.; Tocilescu, M. A.; Liu, W.; Ko, H. S.; Magrane, J.; Moore, D. J.; Dawson, V. L.; Grailhe, R.; Dawson, T. M.; Li, C.; Tieu, K.; Przedborski, S., PINK1-dependent recruitment of Parkin to mitochondria in mitophagy. *Proceedings of the National Academy of Sciences of the United States of America* 2010, *107*(1), 378-83.
14. Kondapalli, C.; Kazlauskaitė, A.; Zhang, N.; Woodroof, H. I.; Campbell, D. G.; Gourlay, R.; Burchell, L.; Walden, H.; Macartney, T. J.; Deak, M.; Knebel, A.; Alessi, D. R.; Muqit, M. M., PINK1 is activated by mitochondrial membrane potential depolarization and stimulates Parkin E3 ligase activity by phosphorylating Serine 65. *Open biology* 2012, *2*(5), 120080.
15. Shiba-Fukushima, K.; Imai, Y.; Yoshida, S.; Ishihama, Y.; Kanao, T.; Sato, S.; Hattori, N., PINK1-mediated phosphorylation of the Parkin ubiquitin-like domain primes mitochondrial translocation of Parkin and regulates mitophagy. *Scientific reports* 2012, *2*, 1002.
16. Iguchi, M.; Kujuro, Y.; Okatsu, K.; Koyano, F.; Kosako, H.; Kimura, M.; Suzuki, N.; Uchiyama, S.; Tanaka, K.; Matsuda, N., Parkin-catalyzed ubiquitin-ester transfer is triggered by PINK1-dependent phosphorylation. *The Journal of biological chemistry* 2013, *288*(30), 22019-32.
17. Chaugule, V. K.; Burchell, L.; Barber, K. R.; Sidhu, A.; Leslie, S. J.; Shaw, G. S.; Walden, H., Autoregulation of Parkin activity through its ubiquitin-like domain. *The EMBO journal* 2011, *30*(14), 2853-67.
18. Lazarou, M.; Narendra, D. P.; Jin, S. M.; Tekle, E.; Banerjee, S.; Youle, R. J., PINK1 drives Parkin self-association and HECT-like E3 activity upstream of mitochondrial binding. *The Journal of cell biology* 2013, *200*(2), 163-72.

19. Gegg, M. E.; Cooper, J. M.; Chau, K. Y.; Rojo, M.; Schapira, A. H.; Taanman, J. W., Mitofusin 1 and mitofusin 2 are ubiquitinated in a PINK1/parkin-dependent manner upon induction of mitophagy. *Human molecular genetics* 2010, *19*(24), 4861-70.
20. Geisler, S.; Holmstrom, K. M.; Skujat, D.; Fiesel, F. C.; Rothfuss, O. C.; Kahle, P. J.; Springer, W., PINK1/Parkin-mediated mitophagy is dependent on VDAC1 and p62/SQSTM1. *Nature cell biology* 2010, *12*(2), 119-31.
21. Tanaka, A.; Cleland, M. M.; Xu, S.; Narendra, D. P.; Suen, D. F.; Karbowski, M.; Youle, R. J., Proteasome and p97 mediate mitophagy and degradation of mitofusins induced by Parkin. *The Journal of cell biology* 2010, *191*(7), 1367-80.
22. Ziviani, E.; Tao, R. N.; Whitworth, A. J., Drosophila parkin requires PINK1 for mitochondrial translocation and ubiquitinates mitofusin. *Proceedings of the National Academy of Sciences of the United States of America* 2010, *107*(11), 5018-23.
23. Chan, N. C.; Salazar, A. M.; Pham, A. H.; Sweredoski, M. J.; Kolawa, N. J.; Graham, R. L.; Hess, S.; Chan, D. C., Broad activation of the ubiquitin-proteasome system by Parkin is critical for mitophagy. *Human molecular genetics* 2011, *20*(9), 1726-37.
24. Wang, X.; Winter, D.; Ashrafi, G.; Schlehe, J.; Wong, Y. L.; Selkoe, D.; Rice, S.; Steen, J.; LaVoie, M. J.; Schwarz, T. L., PINK1 and Parkin target Miro for phosphorylation and degradation to arrest mitochondrial motility. *Cell* 2011, *147*(4), 893-906.
25. Yoshii, S. R.; Kishi, C.; Ishihara, N.; Mizushima, N., Parkin mediates proteasome-dependent protein degradation and rupture of the outer mitochondrial membrane. *The Journal of biological chemistry* 2011, *286*(22), 19630-40.
26. Liu, S.; Sawada, T.; Lee, S.; Yu, W.; Silverio, G.; Alapatt, P.; Millan, I.; Shen, A.; Saxton, W.; Kanao, T.; Takahashi, R.; Hattori, N.; Imai, Y.; Lu, B., Parkinson's disease-associated kinase PINK1 regulates Miro protein level and axonal transport of mitochondria. *PLoS genetics* 2012, *8*(3), e1002537.
27. Okatsu, K.; Iemura, S.; Koyano, F.; Go, E.; Kimura, M.; Natsume, T.; Tanaka, K.; Matsuda, N., Mitochondrial hexokinase HKI is a novel substrate of the Parkin ubiquitin ligase. *Biochemical and biophysical research communications* 2012, *428*(1), 197-202.
28. Sarraf, S. A.; Raman, M.; Guarani-Pereira, V.; Sowa, M. E.; Huttlin, E. L.; Gygi, S. P.; Harper, J. W., Landscape of the PARKIN-dependent ubiquitylome in response to mitochondrial depolarization. *Nature* 2013, *496*(7445), 372-6.
29. Spratt, D. E.; Walden, H.; Shaw, G. S., RBR E3 ubiquitin ligases: new structures, new insights, new questions. *The Biochemical journal* 2014, *458*(3), 421-37.
30. Wenzel, D. M.; Lissounov, A.; Brzovic, P. S.; Klevit, R. E., UBC7 reactivity profile reveals parkin and HHARI to be RING/HECT hybrids. *Nature* 2011, *474*(7349), 105-8.
31. Sterky, F. H.; Lee, S.; Wibom, R.; Olson, L.; Larsson, N. G., Impaired mitochondrial

transport and Parkin-independent degeneration of respiratory chain-deficient dopamine neurons in vivo. *Proceedings of the National Academy of Sciences of the United States of America* 2011, *108*(31), 12937-42.

32. Koyano, F.; Okatsu, K.; Ishigaki, S.; Fujioka, Y.; Kimura, M.; Sobue, G.; Tanaka, K.; Matsuda, N., The principal PINK1 and Parkin cellular events triggered in response to dissipation of mitochondrial membrane potential occur in primary neurons. *Genes to cells* : 2013, *18*(8), 672-81.

33. Narendra, D.; Walker, J. E.; Youle, R., Mitochondrial quality control mediated by PINK1 and Parkin: links to parkinsonism. *Cold Spring Harbor perspectives in biology* 2012, *4*(11).

34. Koyano, F.; Okatsu, K.; Kosako, H.; Tamura, Y.; Go, E.; Kimura, M.; Kimura, Y.; Tsuchiya, H.; Yoshihara, H.; Hirokawa, T.; Endo, T.; Fon, E. A.; Trempe, J. F.; Saeki, Y.; Tanaka, K.; Matsuda, N., Ubiquitin is phosphorylated by PINK1 to activate parkin. *Nature* 2014, *510*(7503), 162-6.

35. Campeau, E.; Ruhl, V. E.; Rodier, F.; Smith, C. L.; Rahmberg, B. L.; Fuss, J. O.; Campisi, J.; Yaswen, P.; Cooper, P. K.; Kaufman, P. D., A versatile viral system for expression and depletion of proteins in mammalian cells. *PloS one* 2009, *4*(8), e6529.

36. Tsuchiya, H.; Tanaka, K.; Saeki, Y., The parallel reaction monitoring method contributes to a highly sensitive polyubiquitin chain quantification. *Biochemical and biophysical research communications* 2013, *436*(2), 223-9.

37. Kinoshita, E.; Kinoshita-Kikuta, E.; Takiyama, K.; Koike, T., Phosphate-binding tag, a new tool to visualize phosphorylated proteins. *Molecular & cellular proteomics : MCP* 2006, *5*(4), 749-57.

38. Narendra, D.; Tanaka, A.; Suen, D. F.; Youle, R. J., Parkin is recruited selectively to impaired mitochondria and promotes their autophagy. *The Journal of cell biology* 2008, *183*(5), 795-803.

39. Van Laar, V. S.; Arnold, B.; Cassady, S. J.; Chu, C. T.; Burton, E. A.; Berman, S. B., Bioenergetics of neurons inhibit the translocation response of Parkin following rapid mitochondrial depolarization. *Human molecular genetics* 2011, *20*(5), 927-40.

40. Cai, Q.; Zakaria, H. M.; Simone, A.; Sheng, Z. H., Spatial parkin translocation and degradation of damaged mitochondria via mitophagy in live cortical neurons. *Current biology : CB* 2012, *22*(6), 545-52.

41. Joselin, A. P.; Hewitt, S. J.; Callaghan, S. M.; Kim, R. H.; Chung, Y. H.; Mak, T. W.; Shen, J.; Slack, R. S.; Park, D. S., ROS-dependent regulation of Parkin and DJ-1 localization during oxidative stress in neurons. *Human molecular genetics* 2012, *21*(22), 4888-903.

42. Matsuda, N.; Kitami, T.; Suzuki, T.; Mizuno, Y.; Hattori, N.; Tanaka, K., Diverse

- effects of pathogenic mutations of Parkin that catalyze multiple monoubiquitylation in vitro. *The Journal of biological chemistry* 2006, *281* (6), 3204-9.
43. Okatsu, K.; Saisho, K.; Shimanuki, M.; Nakada, K.; Shitara, H.; Sou, Y. S.; Kimura, M.; Sato, S.; Hattori, N.; Komatsu, M.; Tanaka, K.; Matsuda, N., p62/SQSTM1 cooperates with Parkin for perinuclear clustering of depolarized mitochondria. *Genes to cells* 2010, *15* (8), 887-900.
  44. Poole, A. C.; Thomas, R. E.; Yu, S.; Vincow, E. S.; Pallanck, L., The mitochondrial fusion-promoting factor mitofusin is a substrate of the PINK1/parkin pathway. *PloS one* 2010, *5* (4), e10054.
  45. Glauser, L.; Sonnay, S.; Stafa, K.; Moore, D. J., Parkin promotes the ubiquitination and degradation of the mitochondrial fusion factor mitofusin 1. *Journal of neurochemistry* 2011, *118* (4), 636-45.
  46. Rakovic, A.; Grunewald, A.; Kottwitz, J.; Bruggemann, N.; Pramstaller, P. P.; Lohmann, K.; Klein, C., Mutations in PINK1 and Parkin impair ubiquitination of Mitofusins in human fibroblasts. *PloS one* 2011, *6* (3), e16746.
  47. Sakata, E.; Yamaguchi, Y.; Kurimoto, E.; Kikuchi, J.; Yokoyama, S.; Yamada, S.; Kawahara, H.; Yokosawa, H.; Hattori, N.; Mizuno, Y.; Tanaka, K.; Kato, K., Parkin binds the Rpn10 subunit of 26S proteasomes through its ubiquitin-like domain. *EMBO reports* 2003, *4* (3), 301-6.
  48. Zheng, X.; Hunter, T., Parkin mitochondrial translocation is achieved through a novel catalytic activity coupled mechanism. *Cell research* 2013, *23* (7), 886-97.
  49. Okatsu, K.; Uno, M.; Koyano, F.; Go, E.; Kimura, M.; Oka, T.; Tanaka, K.; Matsuda, N., A dimeric PINK1-containing complex on depolarized mitochondria stimulates Parkin recruitment. *The Journal of biological chemistry* 2013, *288* (51), 36372-84.
  50. Gautier, C. A.; Kitada, T.; Shen, J., Loss of PINK1 causes mitochondrial functional defects and increased sensitivity to oxidative stress. *Proceedings of the National Academy of Sciences of the United States of America* 2008, *105* (32), 11364-9.
  51. Trempe, J. F.; Sauve, V.; Grenier, K.; Seirafi, M.; Tang, M. Y.; Menade, M.; Al-Abdul-Wahid, S.; Krett, J.; Wong, K.; Kozlov, G.; Nagar, B.; Fon, E. A.; Gehring, K., Structure of parkin reveals mechanisms for ubiquitin ligase activation. *Science* 2013, *340* (6139), 1451-5.
  52. Ciechanover, A.; Hod, Y.; Hershko, A., A heat-stable polypeptide component of an ATP-dependent proteolytic system from reticulocytes. 1978. *Biochemical and biophysical research communications* 2012, *425* (3), 565-70.
  53. Navarro, A.; Boveris, A.; Bandez, M. J.; Sanchez-Pino, M. J.; Gomez, C.; Muntane, G.; Ferrer, I., Human brain cortex: mitochondrial oxidative damage and adaptive response

in Parkinson disease and in dementia with Lewy bodies. *Free radical biology & medicine* 2009, *46*(12), 1574-80.

54. Cotto-Rios, X. M.; Bekes, M.; Chapman, J.; Ueberheide, B.; Huang, T. T., Deubiquitinases as a signaling target of oxidative stress. *Cell reports* 2012, *2*(6), 1475-84.

55. Kulathu, Y.; Garcia, F. J.; Mevissen, T. E.; Busch, M.; Arnaudo, N.; Carroll, K. S.; Barford, D.; Komander, D., Regulation of A20 and other OTU deubiquitinases by reversible oxidation. *Nature communications* 2013, *4*, 1569.

56. Lee, J. G.; Baek, K.; Soetandyo, N.; Ye, Y., Reversible inactivation of deubiquitinases by reactive oxygen species in vitro and in cells. *Nature communications* 2013, *4*, 1568.

57. Riley, B. E.; Loughheed, J. C.; Callaway, K.; Velasquez, M.; Brecht, E.; Nguyen, L.; Shaler, T.; Walker, D.; Yang, Y.; Regnstrom, K.; Diep, L.; Zhang, Z.; Chiou, S.; Bova, M.; Artis, D. R.; Yao, N.; Baker, J.; Yednock, T.; Johnston, J. A., Structure and function of Parkin E3 ubiquitin ligase reveals aspects of RING and HECT ligases. *Nature communications* 2013, *4*, 1982.

58. Wauer, T.; Komander, D., Structure of the human Parkin ligase domain in an autoinhibited state. *The EMBO journal* 2013, *32*(15), 2099-112.

59. Spratt, D. E.; Martinez-Torres, R. J.; Noh, Y. J.; Mercier, P.; Manczyk, N.; Barber, K. R.; Aguirre, J. D.; Burchell, L.; Purkiss, A.; Walden, H.; Shaw, G. S., A molecular explanation for the recessive nature of parkin-linked Parkinson's disease. *Nature communications* 2013, *4*, 1983.

60. Schapira, A. H., Complex I: inhibitors, inhibition and neurodegeneration. *Experimental neurology* 2010, *224*(2), 331-5.

61. Kinoshita, E.; Kinoshita-Kikuta, E.; Koike, T., Phos-tag SDS-PAGE systems for phosphorylation profiling of proteins with a wide range of molecular masses under neutral pH conditions. *Proteomics* 2012, *12*(2), 192-202.

Figure 1. A history of PINK1/Parkin study

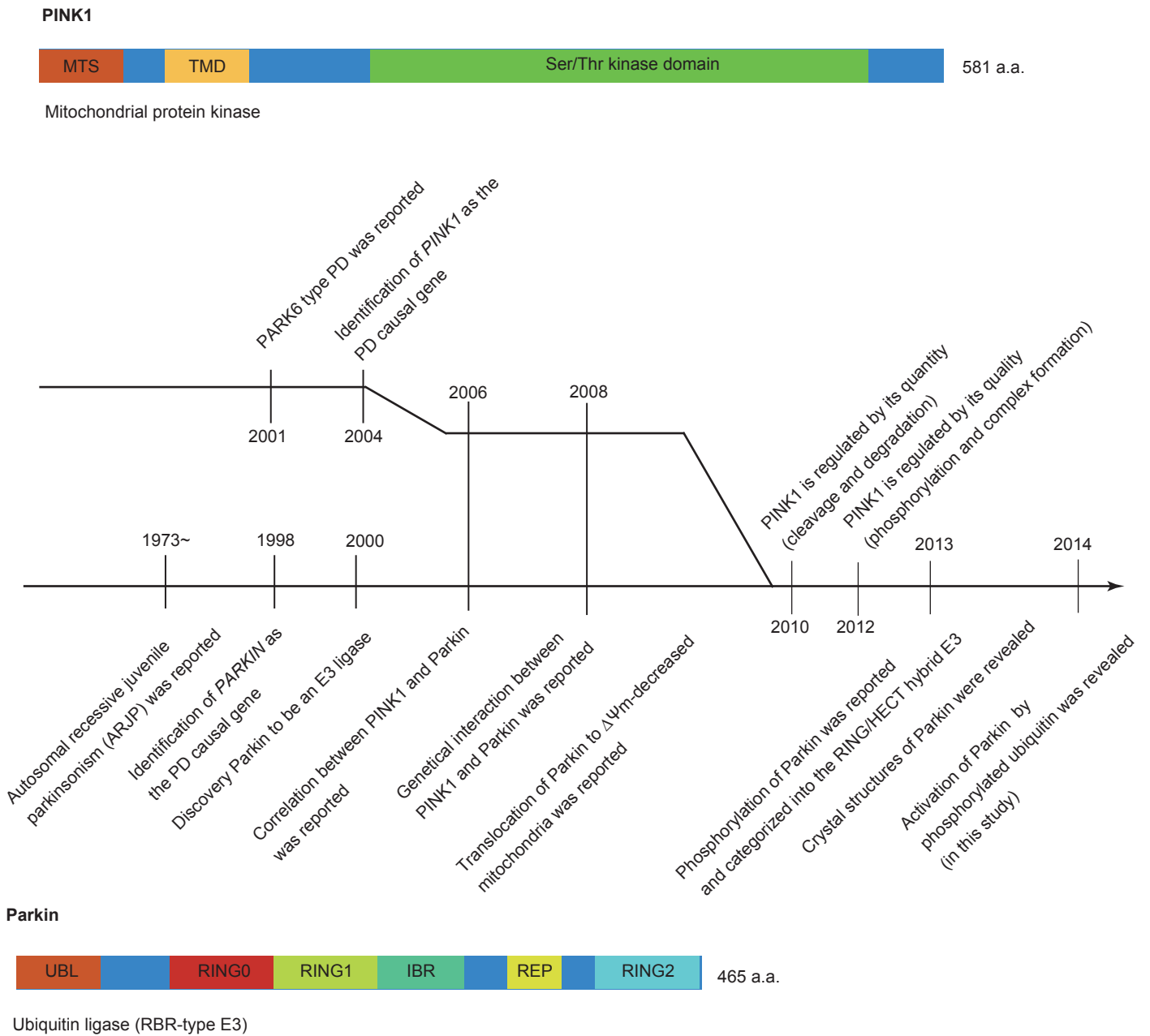


Figure 2. Mitochondrial energetic mechanism and the quality control system

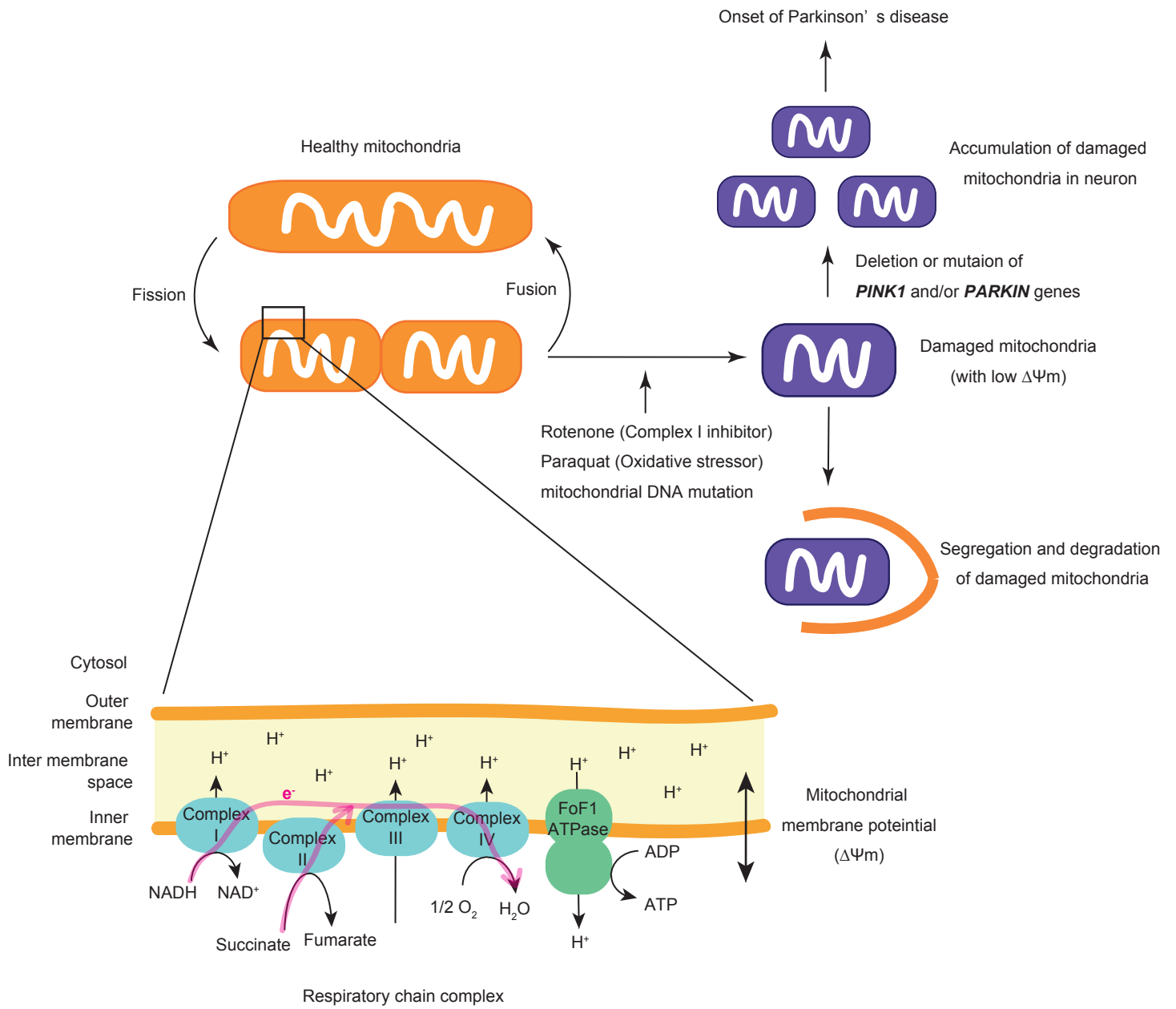


Figure 3 Ubiquitylation and proteolysis systems

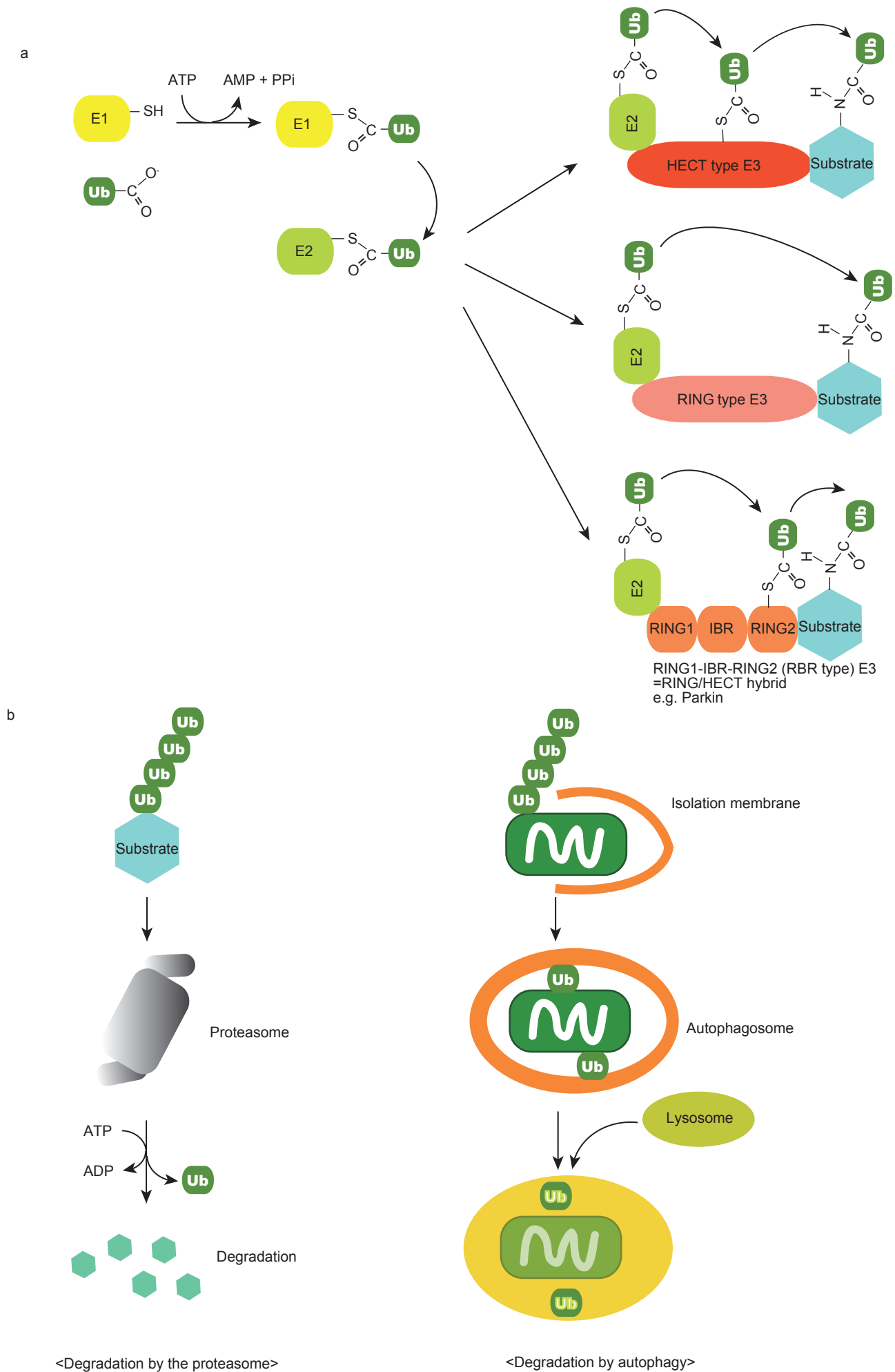


Figure 4.

PINK1 and Parkin are phosphorylated following a decrease in  $\Delta\Psi_m$  in mouse primary neurons.

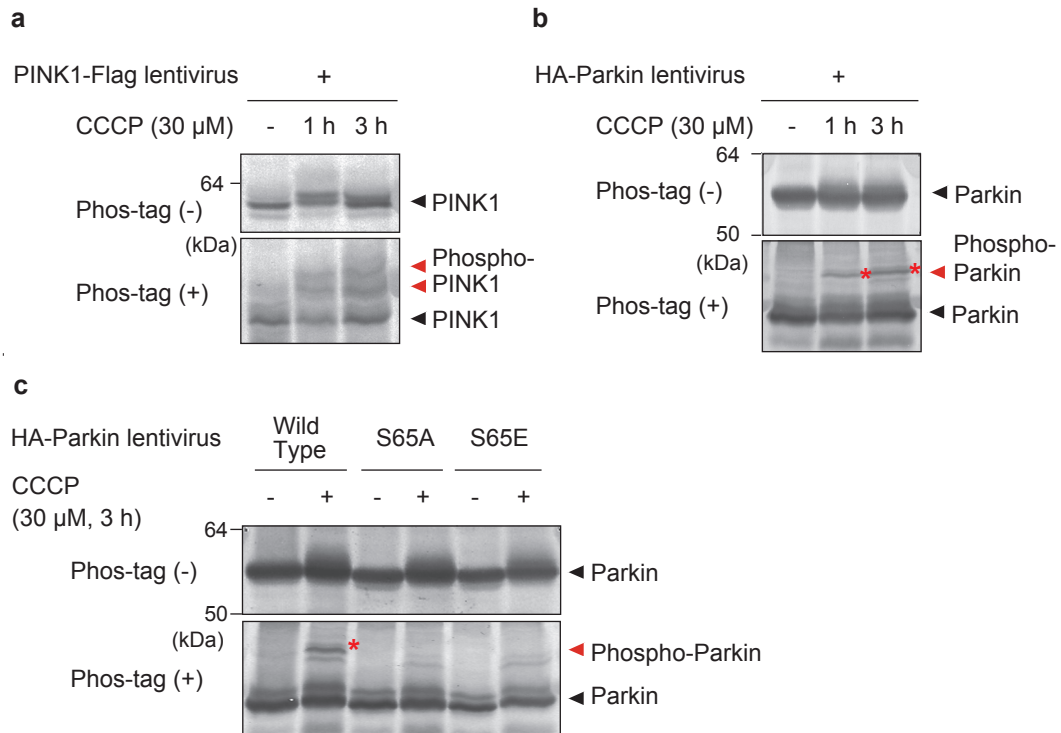


Figure 5. Parkin is recruited to depolarized mitochondria and is activated in neurons.

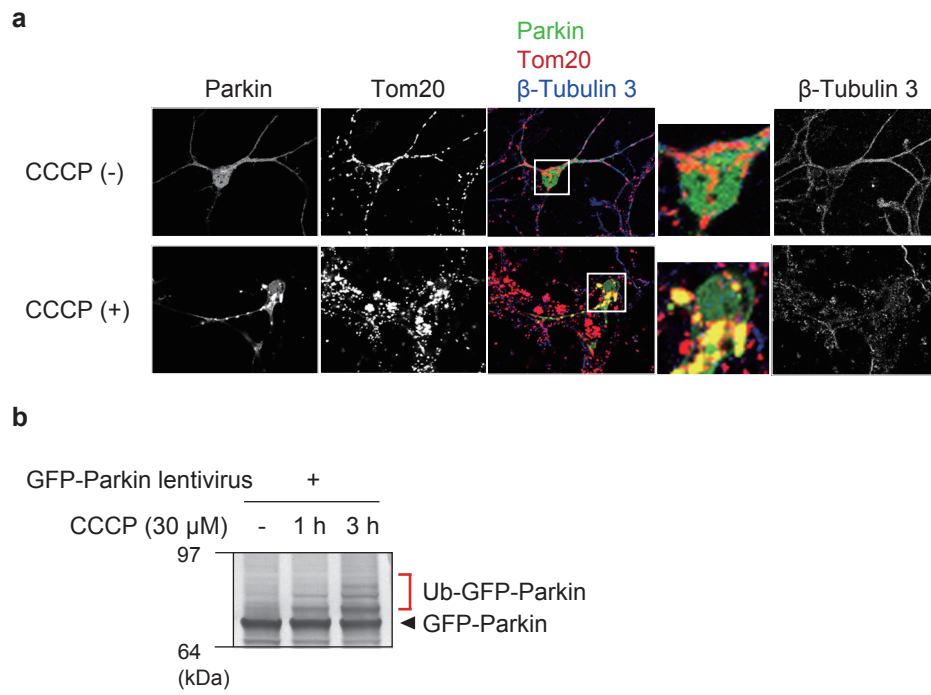
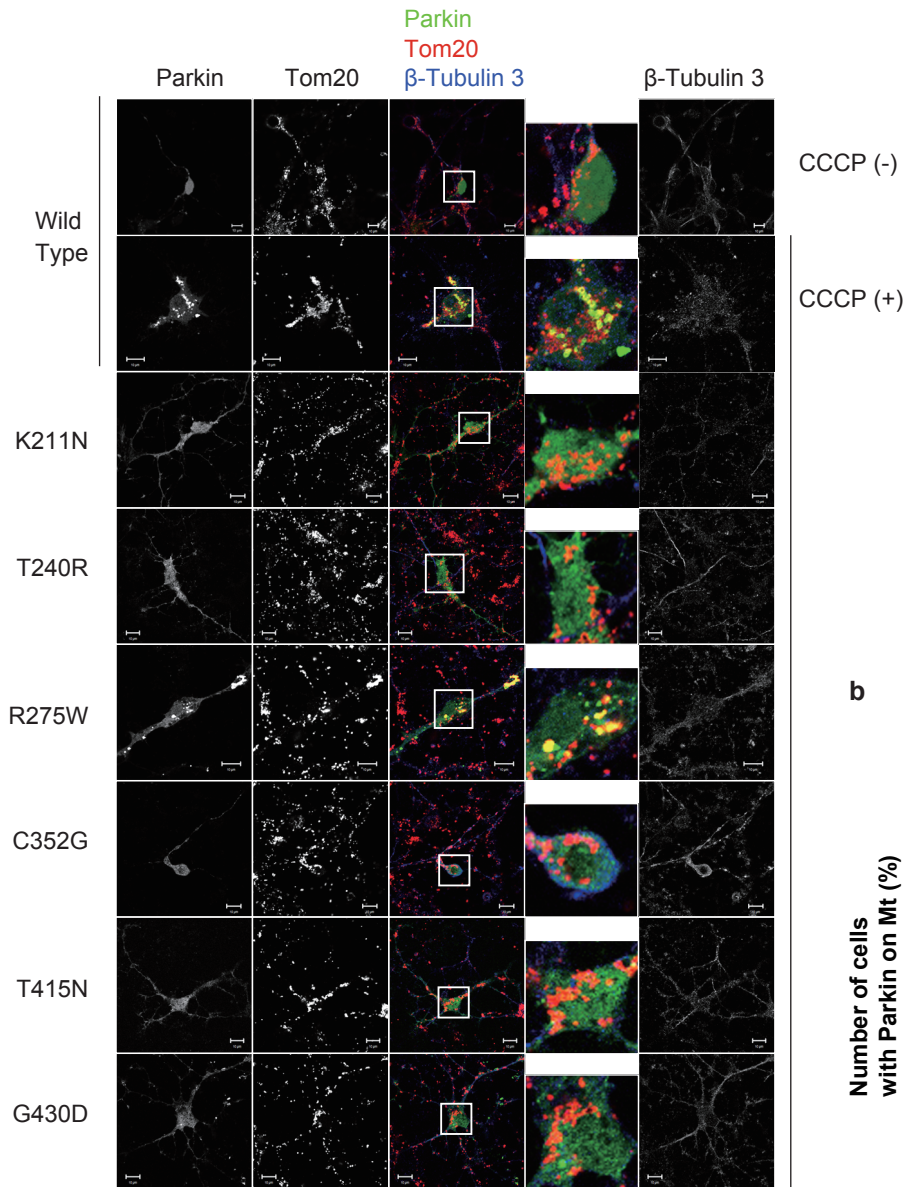


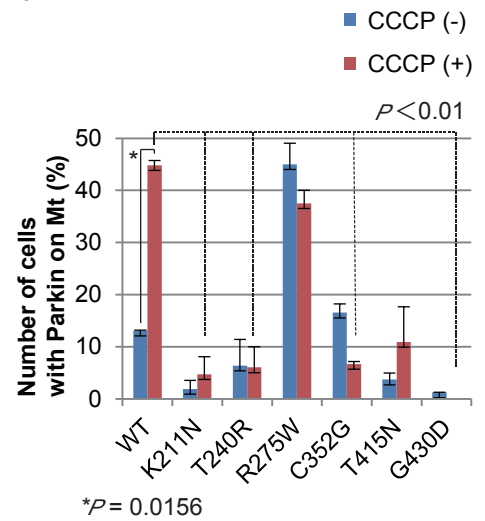
Figure 6.

Disease-relevant Parkin mutations impair mitochondrial localization and E3 activity following CCCP treatment.

**a**



**b**



**c**

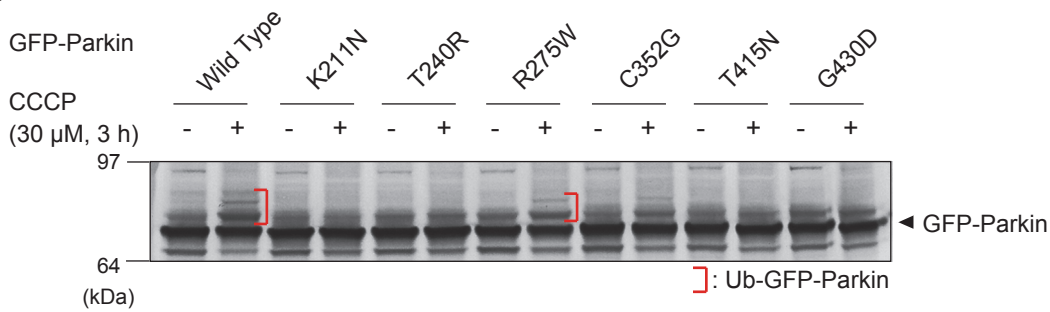


Figure 7.

Several outer-membrane mitochondrial proteins

underwent Parkin-dependent ubiquitylation following a decrease in the  $\Delta\Psi_m$ .

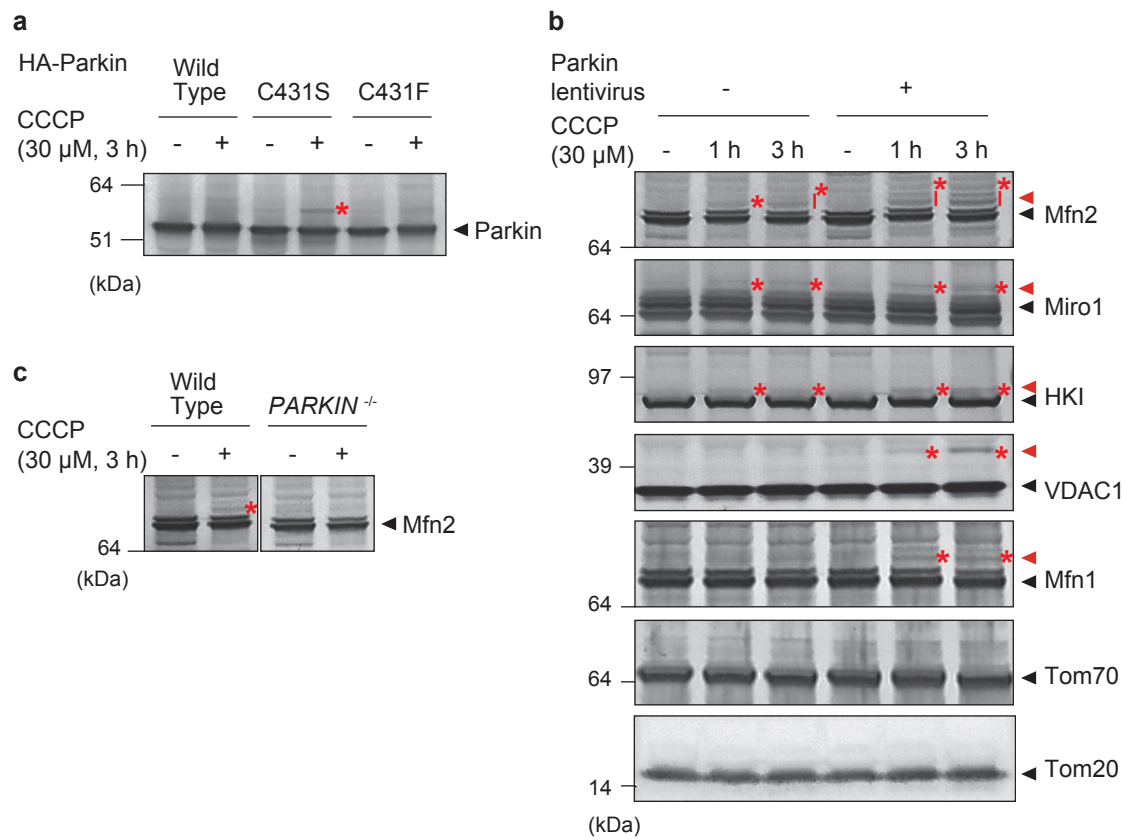




Figure 9. PINK1 phosphorylates ubiquitin.

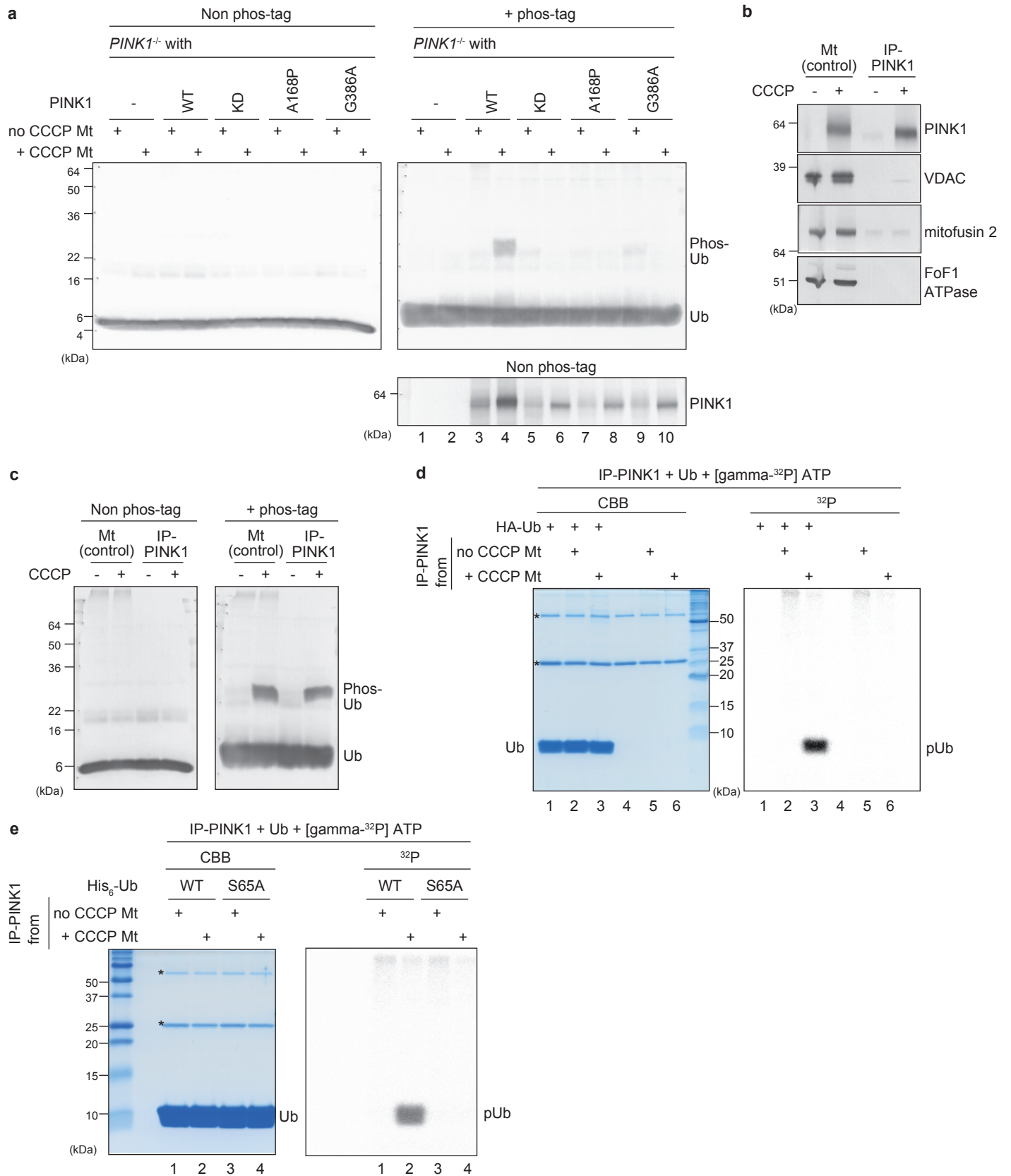
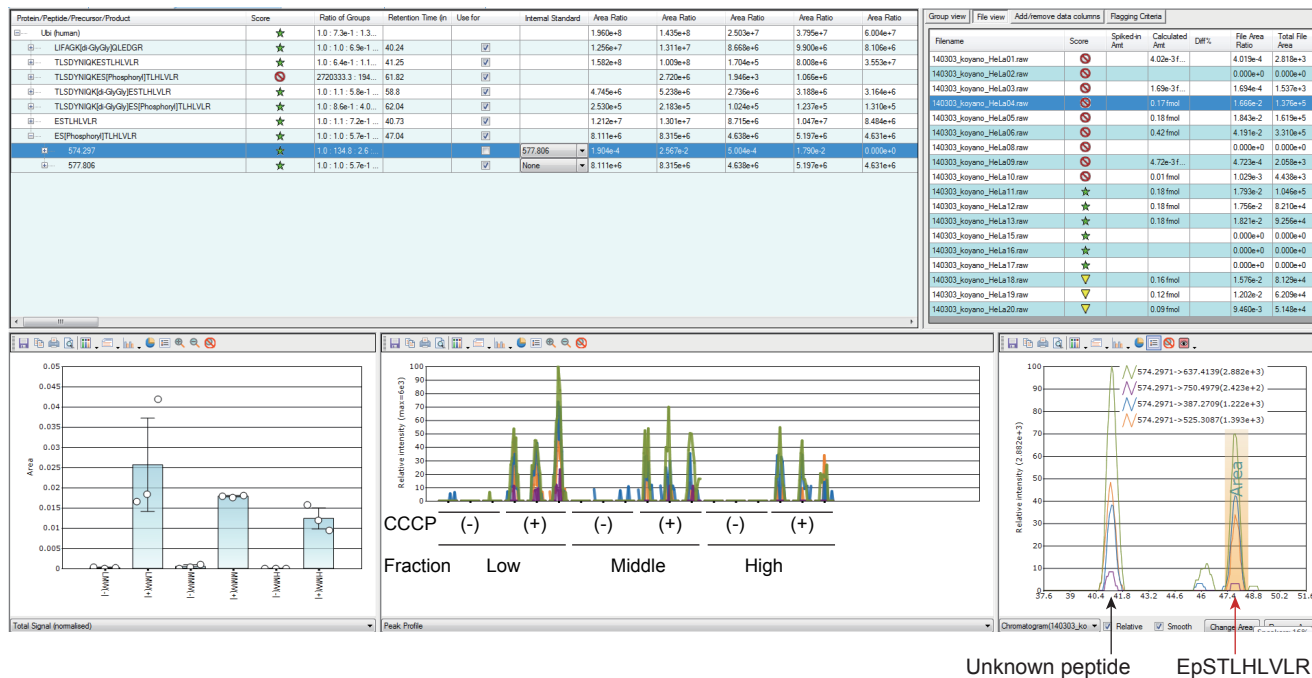


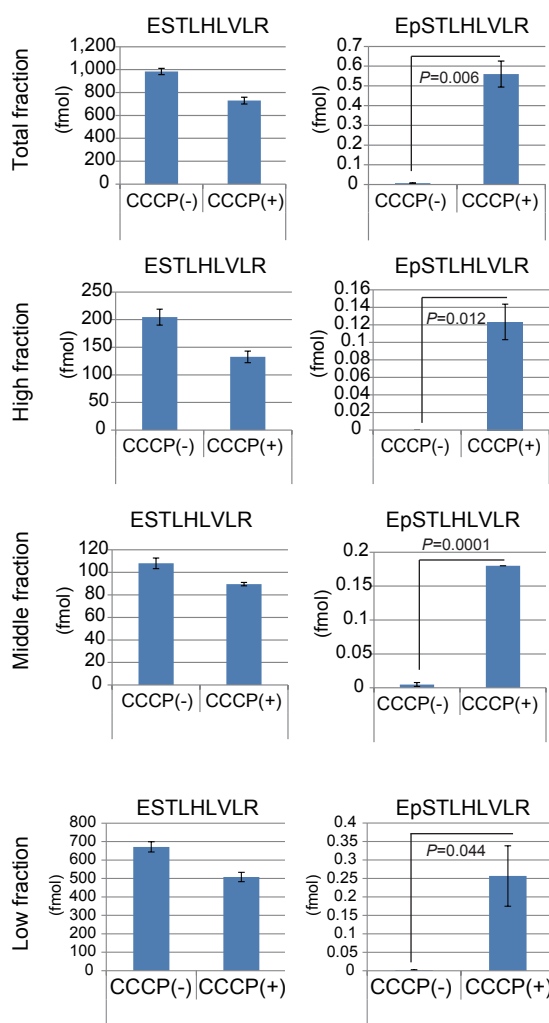
Figure 10.

Mass-spectrometry-based absolute quantification of phosphorylated ubiquitin in intact HeLa cells.

a



b



c

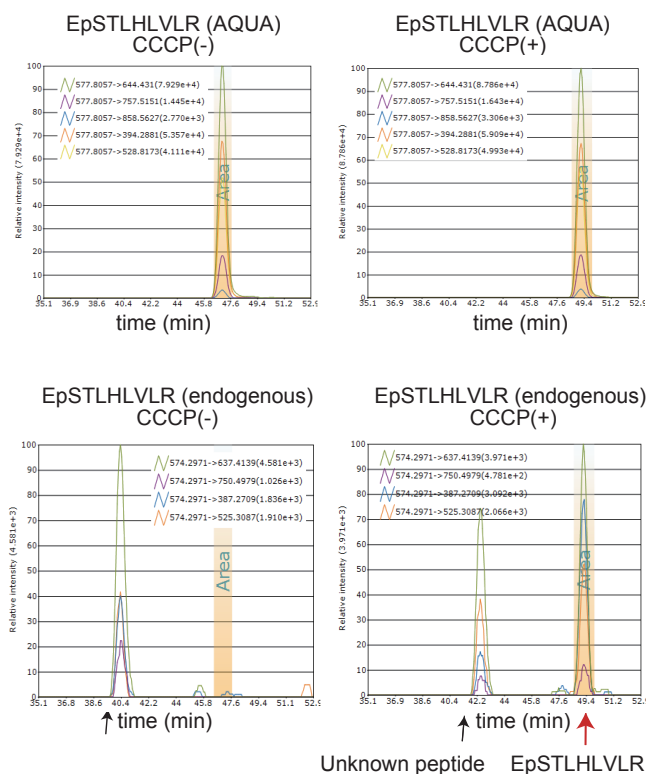


Figure 11. Phosphomimetic ubiquitin activates phosphomimetic Parkin.

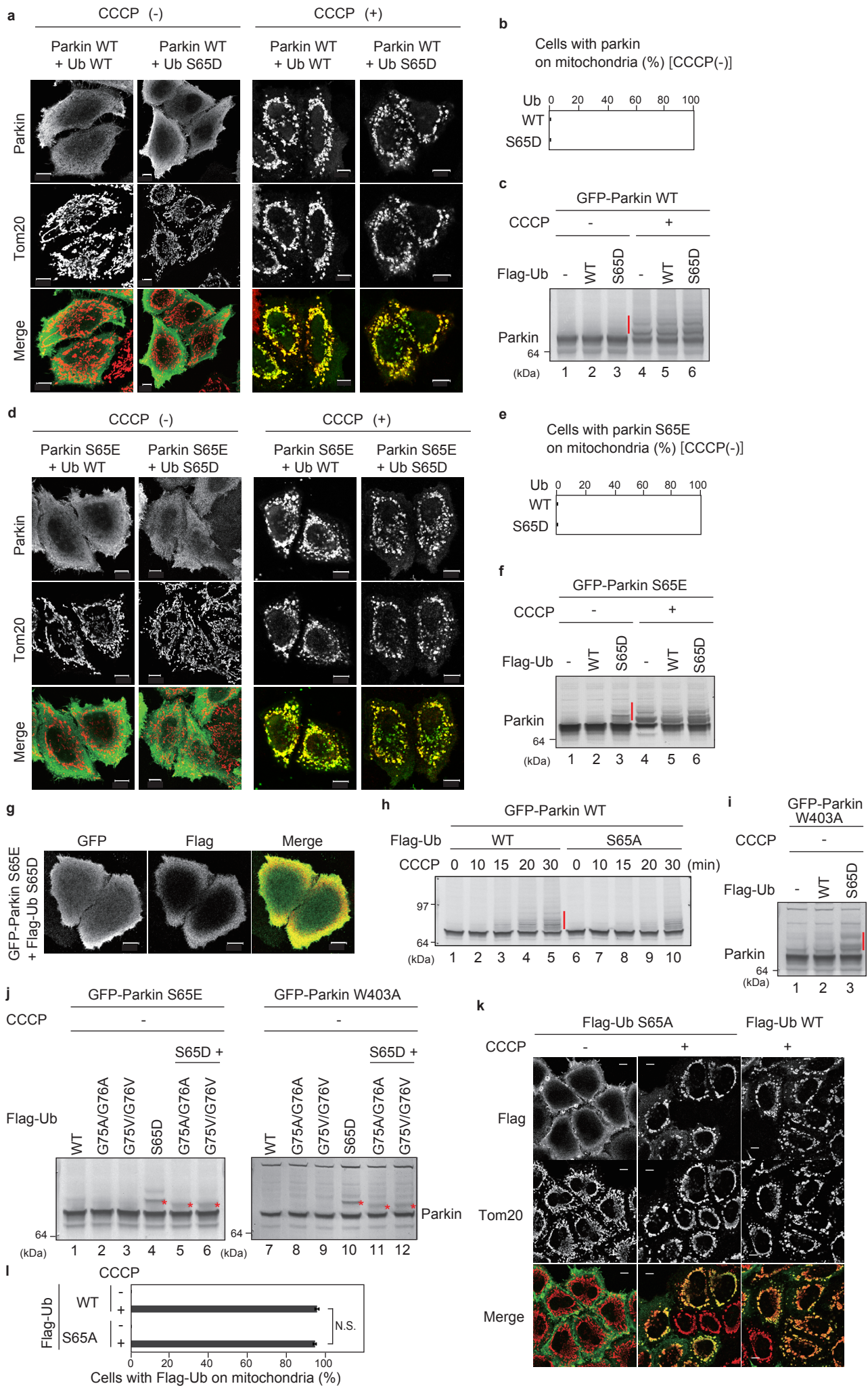


Figure 12.

Subcellular localization of phosphomimetic or phosphorylation-deficient ubiquitin under various experimental conditions.

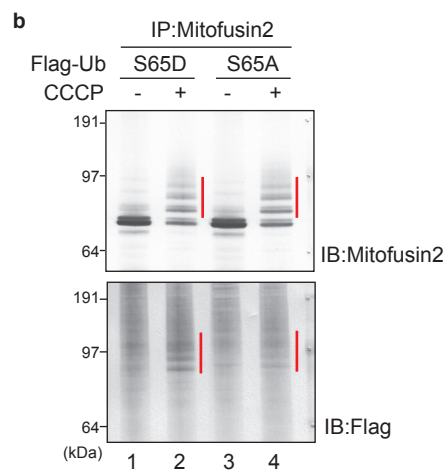
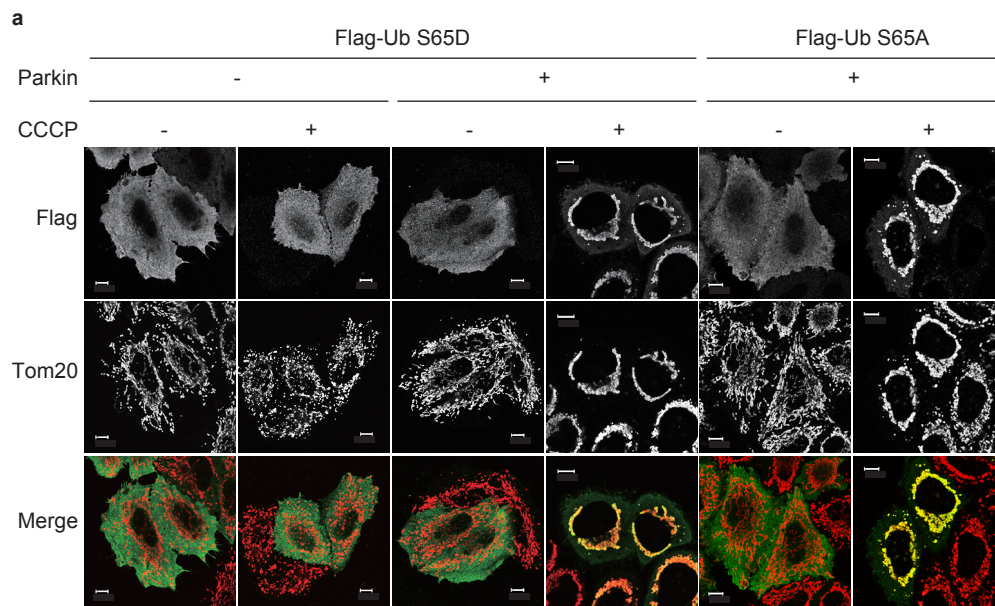


Figure 13. Phosphorylated ubiquitin activates Parkin *in vitro*.

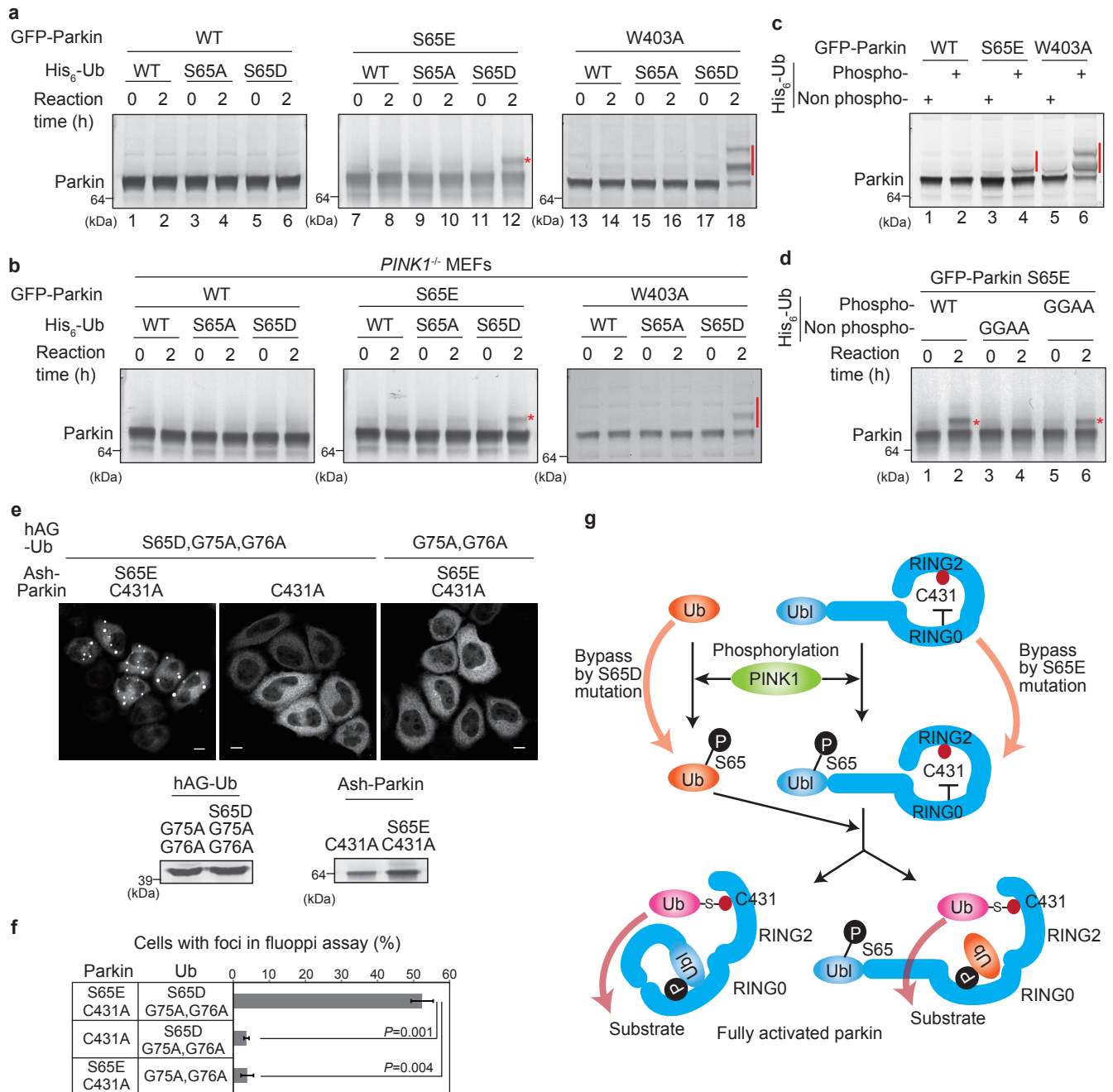


Table 1.

A list of the ubiquitin peptides used in parallel monitoring assay to quantify phosphorylated ubiquitin

Peptide sequence	Precursor m/z (charge state)	Product ions for PRM
ESTLHLVLR	534.314 (+2)	$Y_3^+$ , $Y_4^+$ , $Y_5^+$ , $Y_6^+$ , $Y_7^+$
ESTLHLVL [Heavy] R	537.823 (+2)	$Y_3^+$ , $Y_4^+$ , $Y_5^+$ , $Y_6^+$ , $Y_7^+$
EpSTLHLVLR	574.297 (+2)	$Y_3^+$ , $Y_4^+$ , $Y_5^+$ , $Y_6^+$ , $Y_7^+$
EpSTLHLVL [Heavy] R	577.806 (+2)	$Y_3^+$ , $Y_4^+$ , $Y_5^+$ , $Y_6^+$ , $Y_7^+$